Muon-spin rotation in molecular nanomagnetism

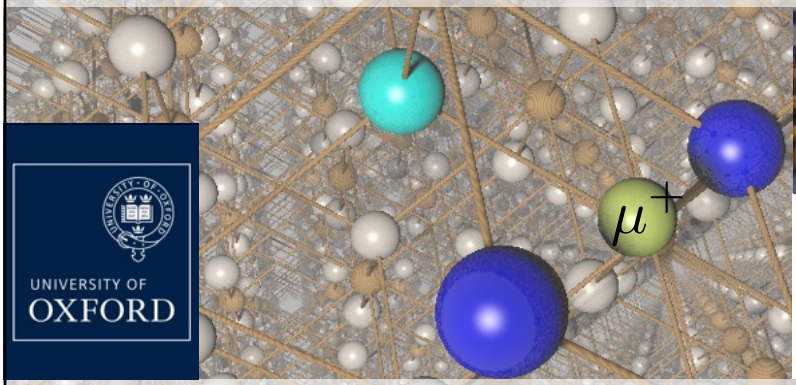

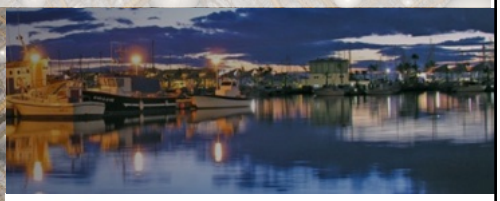

UNIVERSITY OF OXFORD

ESMoINa 2025

Stephen Blundell
University of Oxford, Department of Physics

1

THANKS TO:

Ben M Huddart (Oxford)
Hank CH Wu (Oxford)
Dipranjan Chatterjee (Oxford)
Johannes Moeller (Oxford)
Franz Lang (Oxford)
Jack Wright (Oxford)
Franziska Kirshner

John Wilkinson (Oxford -> ISIS)
Francis L Pratt (ISIS)
Tom Lancaster (Durham)

John Schlueter (Argonne)
Jamie L Manson (Eastern Washington)
D. Prabhakaran (Oxford)
Simon Clarke (Oxford)
Eugenio Coronado (Valencia)

ISIS and PSI for beamtime
EPSRC, ERC, UKRI for funding

erc

MUCONTROL

UK Research and Innovation

2

Magnetic measurements

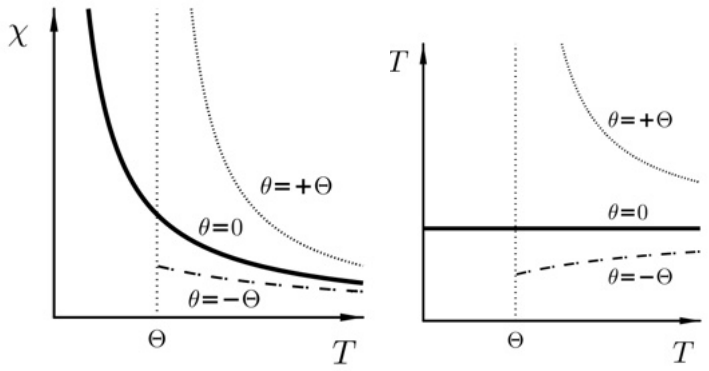

$$\chi = \lim_{\delta H \to 0} \frac{\delta M}{\delta H}$$

$$\langle M \rangle = \frac{1}{V} \int \mathrm{d}^3 r M(\mathbf{r})$$

- Susceptibility should be measured in the limit of vanishing applied field – it never is
- Magnetization is actually a sample average

3

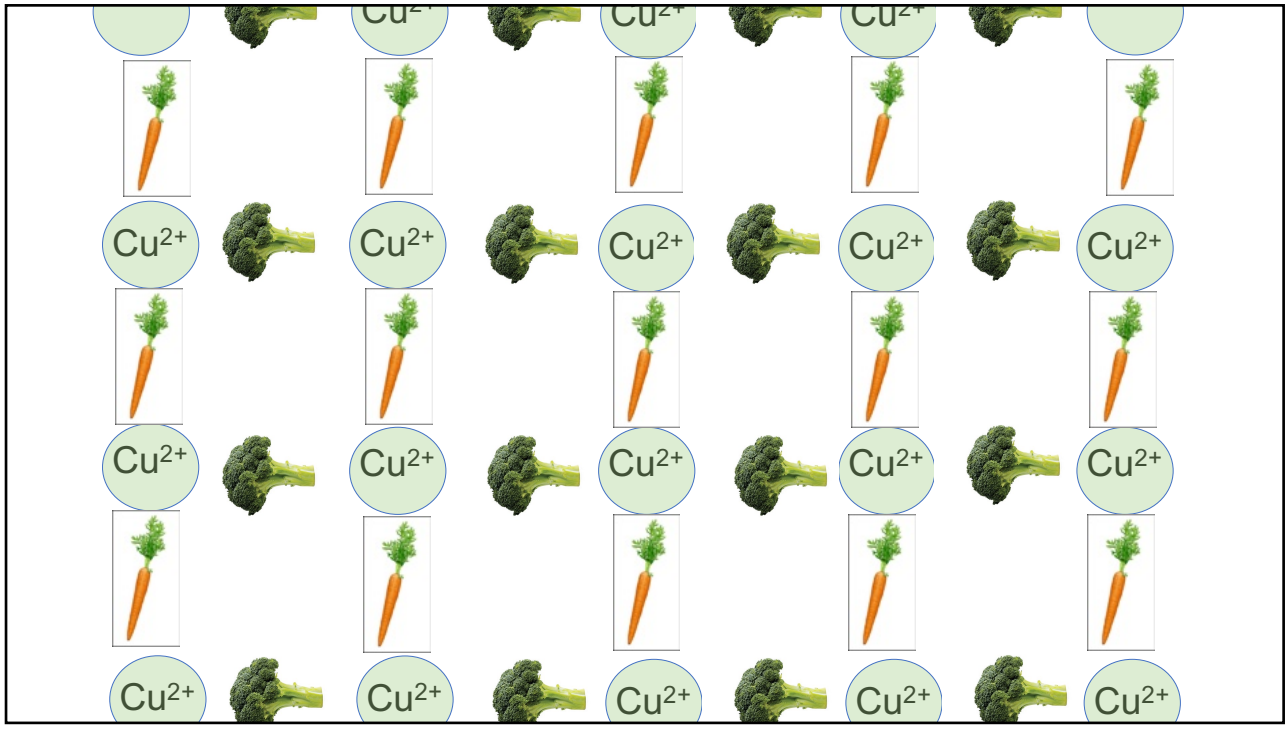

4

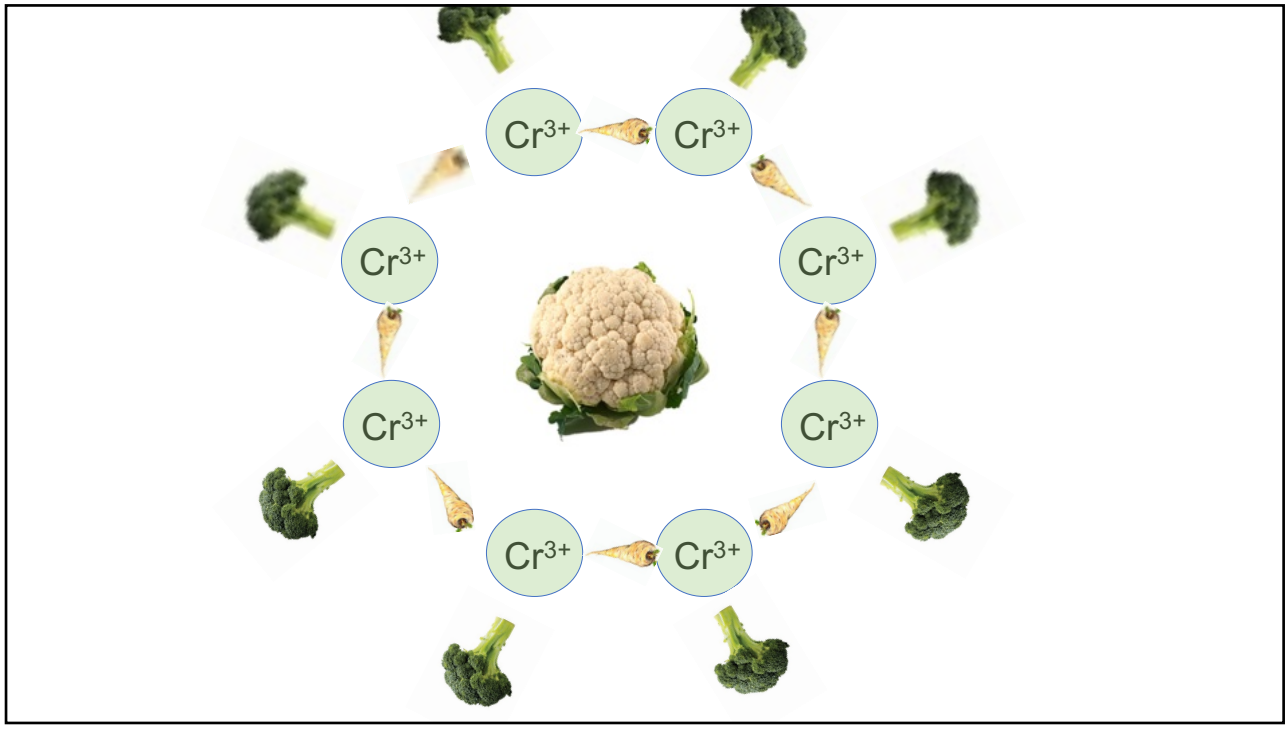

5

Particle physics picture

QUARKS

u	s	t
d	c	b

LEPTONS

e	μ	τ
ν_e	ν_μ	ν_τ

Condensed matter physics picture

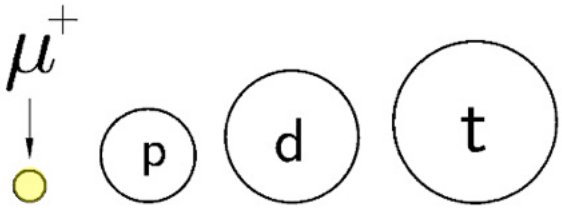

$\frac{1}{9}$: 1 : 2 : 3

6

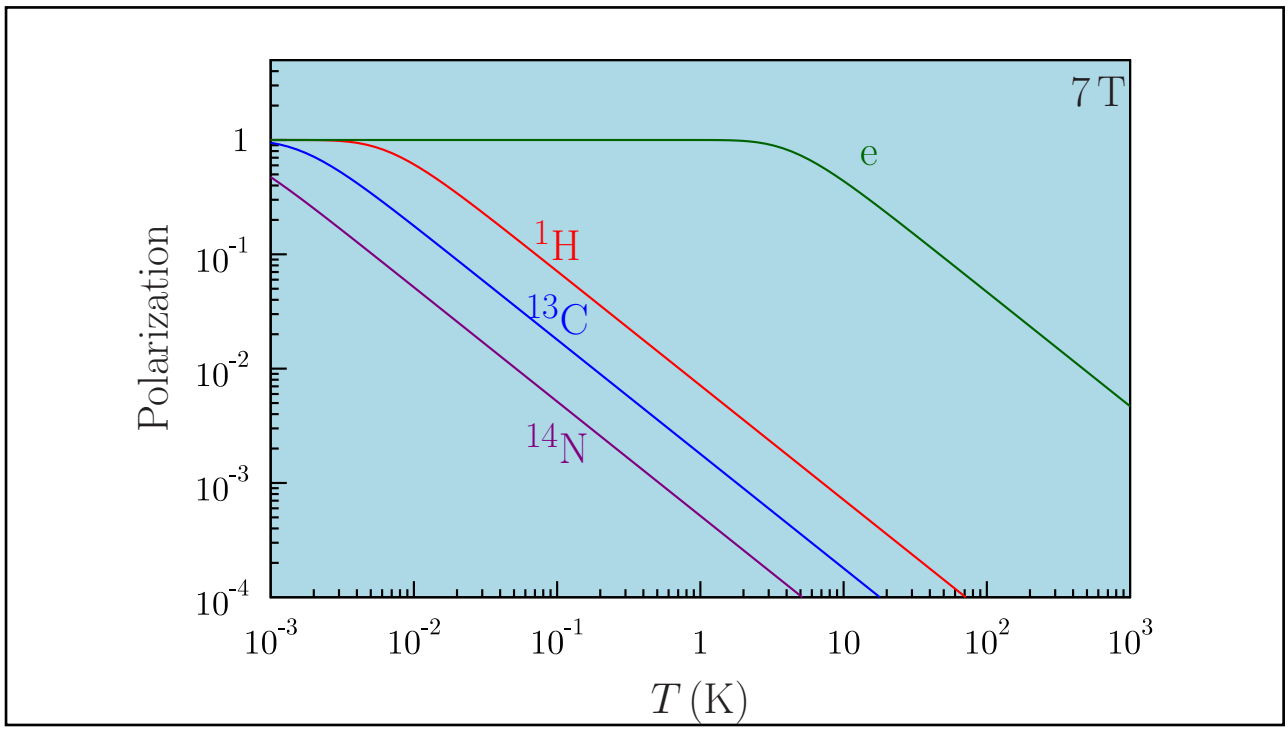
7 T
e
^{1}H
^{13}C
^{14}N
Polarization
1
10^{-1}
10^{-2}
10^{-3}
10^{-4}
10^{-3}
10^{-2}
10^{-1}
1
10
10^{2}
10^{3}
T (K)

7

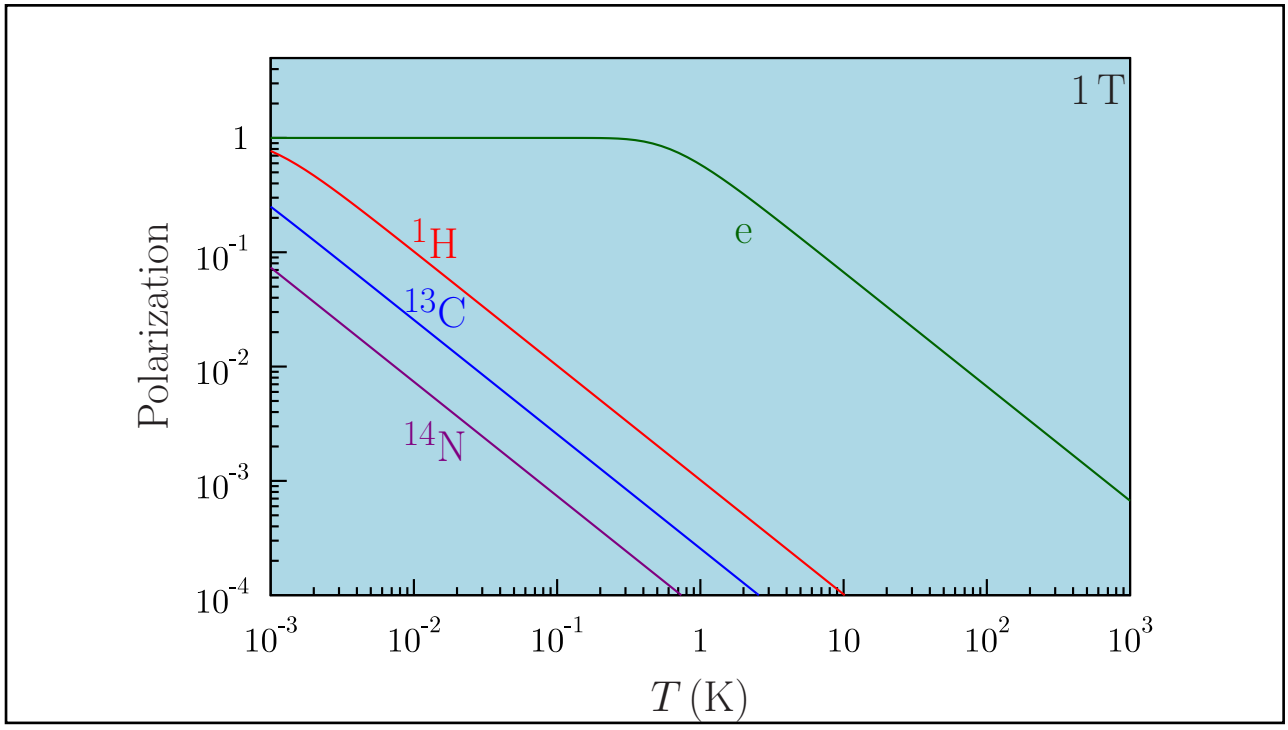
1 T
e
^{1}H
^{13}C
^{14}N
Polarization
1
10^{-1}
10^{-2}
10^{-3}
10^{-4}
10^{-3}
10^{-2}
10^{-1}
1
10
10^{2}
10^{3}
T (K)

8

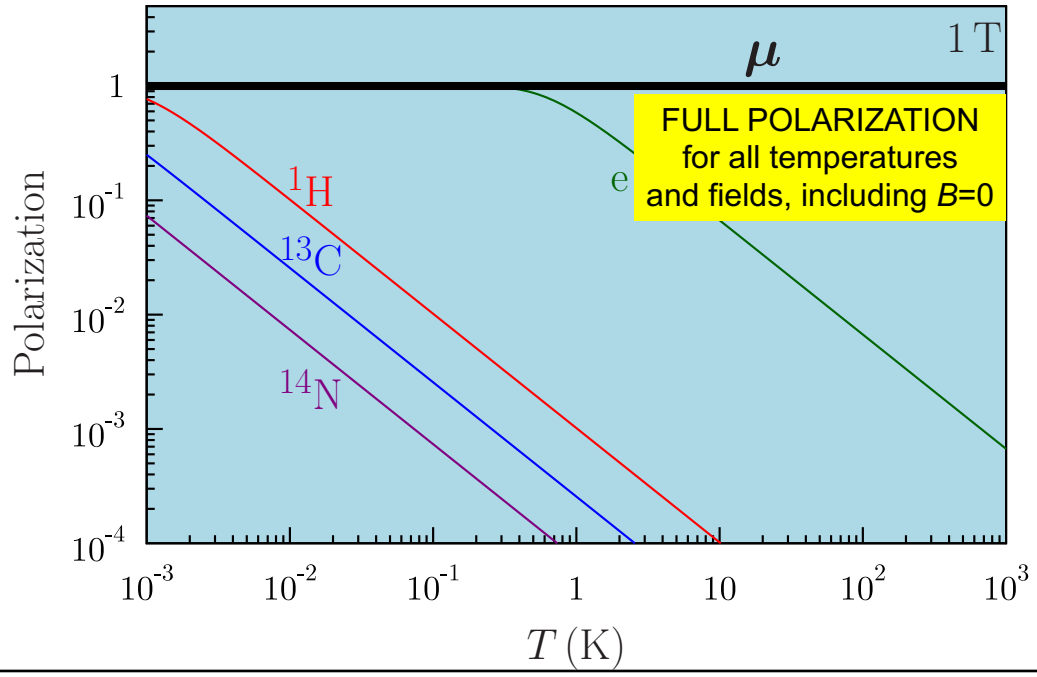

9

	MUON	ELECTRON	PROTON = ^{1}H
property	μ^+	e	p
mass	1.8835×10^{-28} kg	9.1094×10^{-31} kg	1.6726×10^{-27} kg
	105.66 MeV	0.511 00 MeV	938.27 MeV
	$0.1126 m_p$	$m_p/1836.2$	m_p
	$206.768 m_e$	m_e	$1836.2 m_e$
charge	$+e$	$-e$	$+e$
spin	$^1/_2$	$^1/_2$	$^1/_2$
magnetic moment	4.4904×10^{-26} J T^{-1}	-928.48×10^{-26} J T^{-1}	1.4106×10^{-26} J T^{-1}
	$3.1833 \mu_p$	$-658.21 \mu_p$	μ_p
	$8.891 \mu_N$	$-1838.3 \mu_N$	$2.7928 \mu_N$
	$4.842 \times 10^{-3} \mu_B$	$-1.001 \mu_B$	$1.521 \times 10^{-3} \mu_B$
gyromagnetic ratio/(2π)	135.53 MHz T^{-1}	28 024.21 MHz T^{-1}	42.577 MHz T^{-1}
lifetime	$2.197\,03 \times 10^{-6}$ s	$>4 \times 10^{23}$ years	$>2 \times 10^{26}$ years

Muon is spin-1/2

S. J. Blundell, Chem. Rev. **104**, 5717 (2004)

10

MUON ELECTRON PROTON = ^{1}H

property	μ^+	e	p
mass	1.8835×10^{-28} kg 105.66 MeV $0.1126 m_p$ $206.768 m_e$	9.1094×10^{-31} kg 0.511 00 MeV $m_p/1836.2$ m_e	1.6726×10^{-27} kg 938.27 MeV m_p $1836.2 m_e$
charge	$+e$	$-e$	$+e$
spin	$^1/_2$	$^1/_2$	$^1/_2$
magnetic moment	4.4904×10^{-26} J T^{-1} $3.1833 \mu_p$ $8.891 \mu_N$ $4.842 \times 10^{-3} \mu_B$	-928.48×10^{-26} J T^{-1} $-658.21 \mu_p$ $-1838.3 \mu_N$ $-1.001 \mu_B$	1.4106×10^{-26} J T^{-1} μ_p $2.7928 \mu_N$ $1.521 \times 10^{-3} \mu_B$
gyromagnetic ratio/(2π)	135.53 MHz T^{-1}	28 024.21 MHz T^{-1}	42.577 MHz T^{-1}
lifetime	$2.197\,03 \times 10^{-6}$ s	$>4 \times 10^{23}$ years	$>2 \times 10^{26}$ years

Muon is spin-1/2
Muon gyromagnetic ratio is 135.5 MHz/T

S. J. Blundell, Chem. Rev. **104**, 5717 (2004)

11

MUON ELECTRON PROTON = ^{1}H

property	μ^+	e	p
mass	1.8835×10^{-28} kg 105.66 MeV $0.1126 m_p$ $206.768 m_e$	9.1094×10^{-31} kg 0.511 00 MeV $m_p/1836.2$ m_e	1.6726×10^{-27} kg 938.27 MeV m_p $1836.2 m_e$
charge	$+e$	$-e$	$+e$
spin	$^1/_2$	$^1/_2$	$^1/_2$
magnetic moment	4.4904×10^{-26} J T^{-1} $3.1833 \mu_p$ $8.891 \mu_N$ $4.842 \times 10^{-3} \mu_B$	-928.48×10^{-26} J T^{-1} $-658.21 \mu_p$ $-1838.3 \mu_N$ $-1.001 \mu_B$	1.4106×10^{-26} J T^{-1} μ_p $2.7928 \mu_N$ $1.521 \times 10^{-3} \mu_B$
gyromagnetic ratio/(2π)	135.53 MHz T^{-1}	28 024.21 MHz T^{-1}	42.577 MHz T^{-1}
lifetime	$2.197\,03 \times 10^{-6}$ s	$>4 \times 10^{23}$ years	$>2 \times 10^{26}$ years

Muon is spin-1/2
Muon gyromagnetic ratio is 135.5 MHz/T
Muon lifetime is 2.2 μs

S. J. Blundell, Chem. Rev. **104**, 5717 (2004)

12

Muons are obtained at accelerators (synchrotrons/cyclotrons) from proton beam colliding with a low Z (carbon) target.

This produces pions, which decay very quickly (26 ns) into a muon and a neutrino.

Postively charged pions stopped in the target have zero momentum and zero spin.

Neutrinos have their spin antiparallel to their momentum.

Therefore, the muons are emitted with their spin antiparallel to the momentum.

THIS YIELDS 100% SPIN-POLARISED MUON BEAMS

S. J. Blundell, Chem. Rev. **104**, 5717 (2004)

13

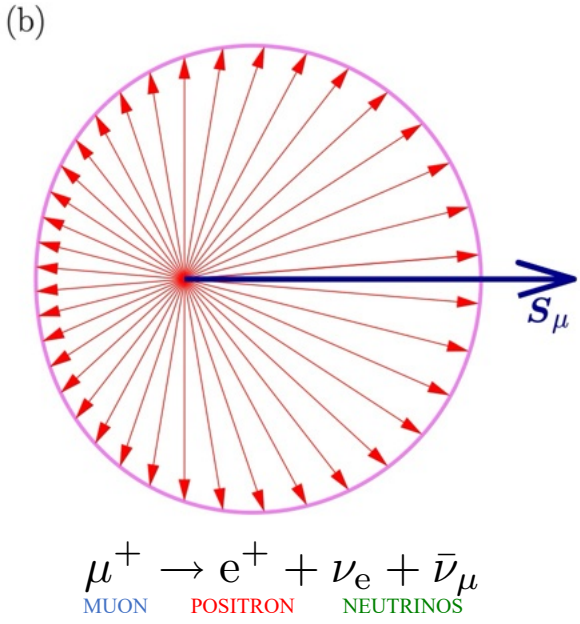

Positive muons decay into positrons.

The positrons are emitted asymmetrically, and are preferentially emitted in the direction of the muon spin (due to violation of parity).

Detecting the angular distribution of the positron decay allows you to infer the direction of the muon spin.

S. J. Blundell, Chem. Rev. **104**, 5717 (2004)

14

Observations of the Failure of Conservation of Parity and Charge Conjugation in Meson Decays: the Magnetic Moment of the Free Muon*

RICHARD L. GARWIN,† LEON M. LEDERMAN, AND MARCEL WEINRICH

Physics Department, Nevis Cyclotron Laboratories, Columbia University, Irvington-on-Hudson, New York, New York

(Received January 15, 1957)

Richard Garwin
(1928-2025)

Leon Lederman
(1922-2018)

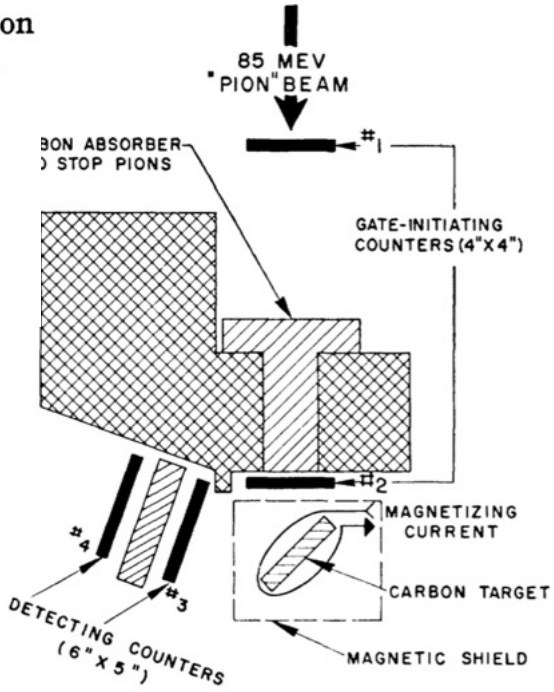

15

"How we violated parity in a weekend .. and discovered God"

Leon Lederman – *The God Particle*

Richard Garwin
(1928-2025)

Leon Lederman
(1922-2018)

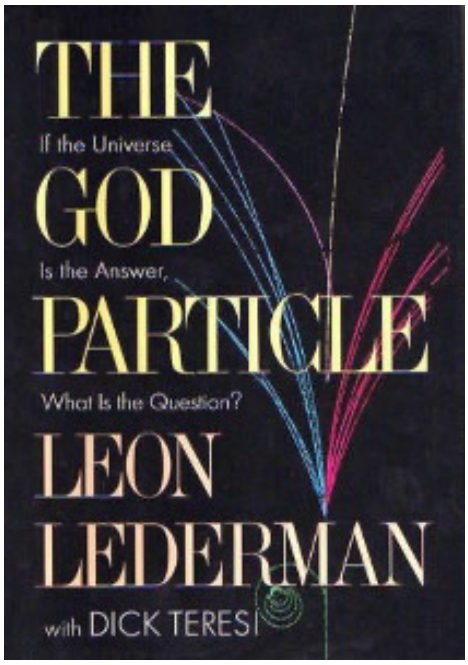

16

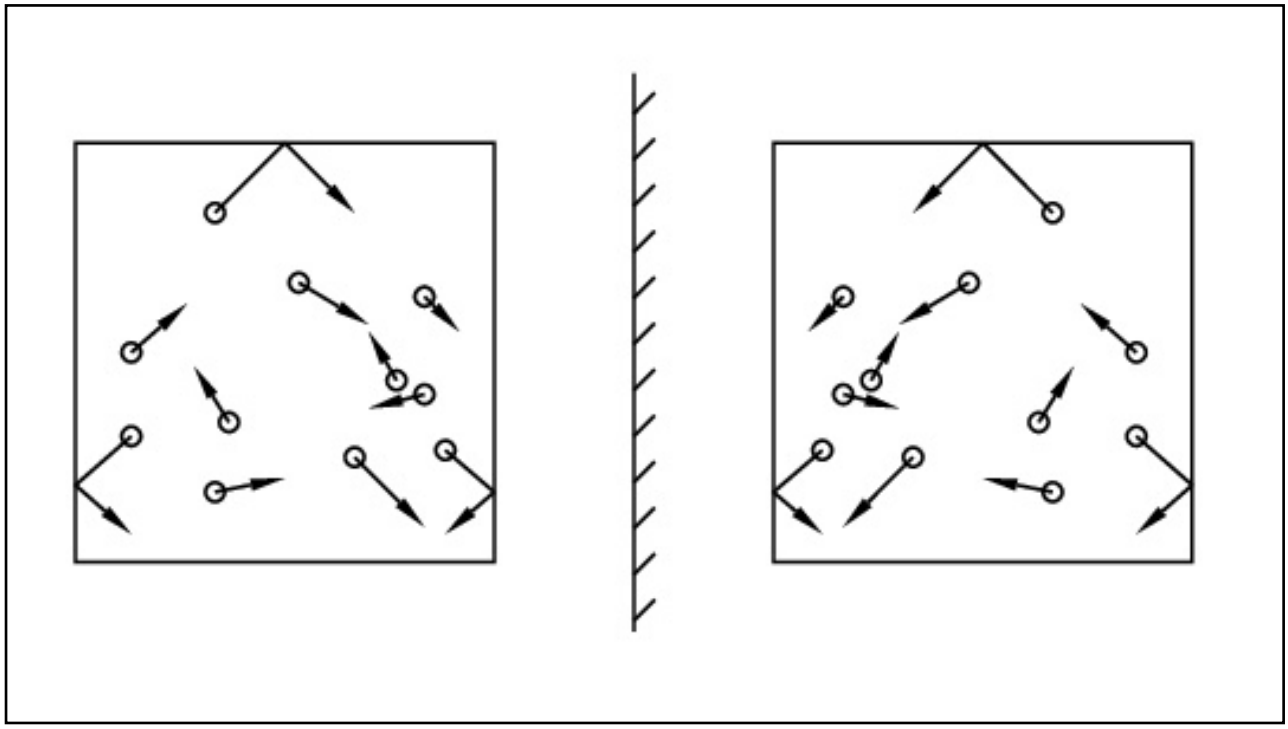

17

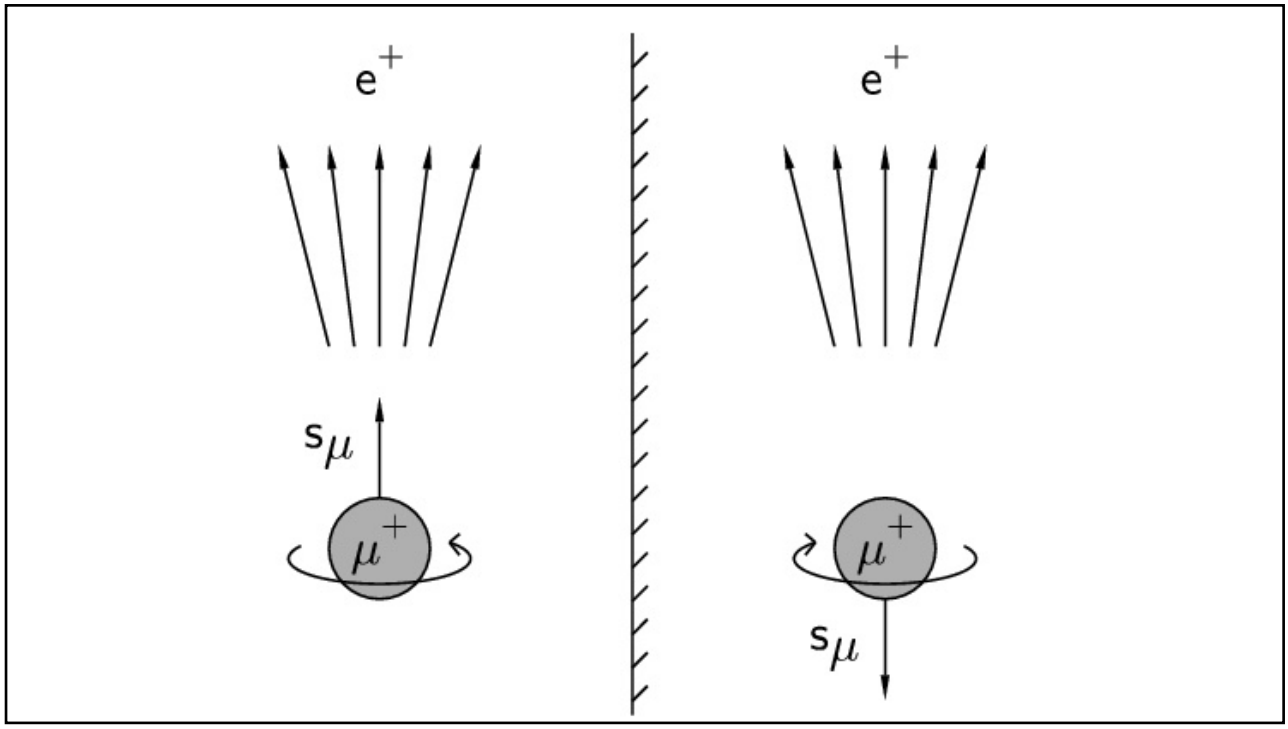

18

"I cannot believe God is a weak left-hander"

Wolfgang Pauli
(1900-1958)

19

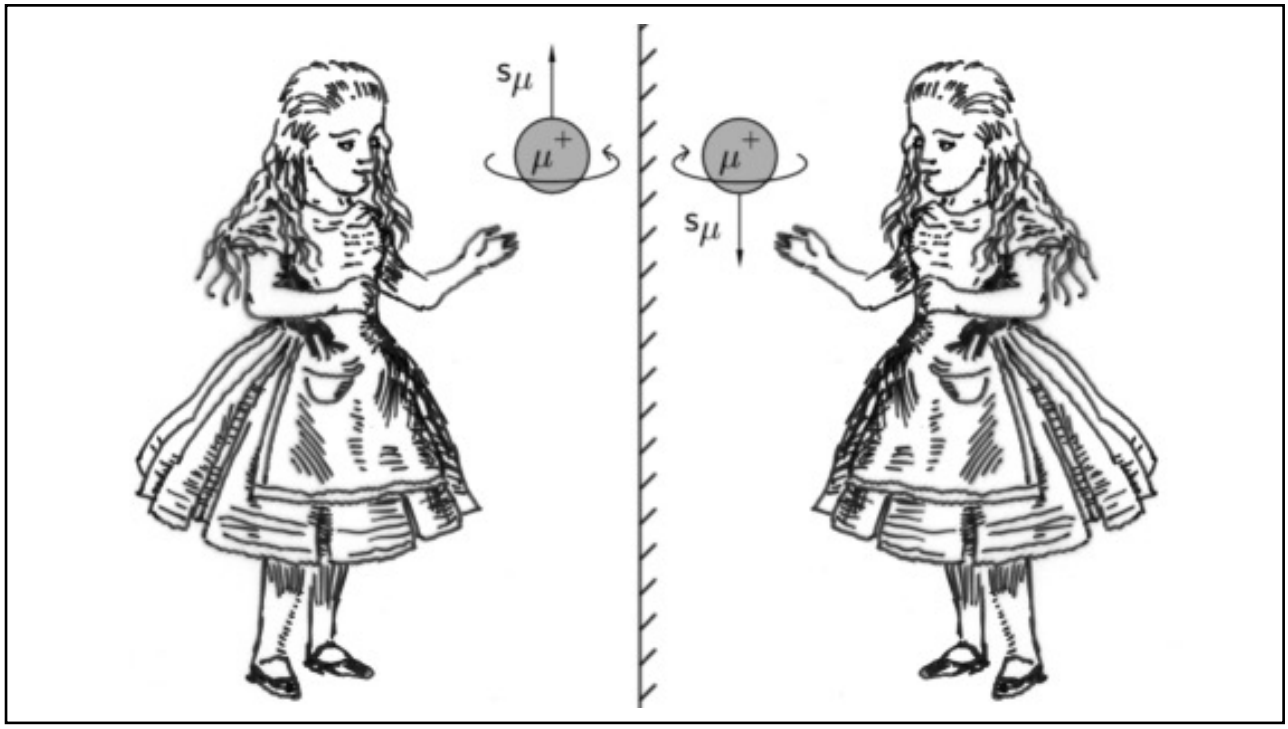

20

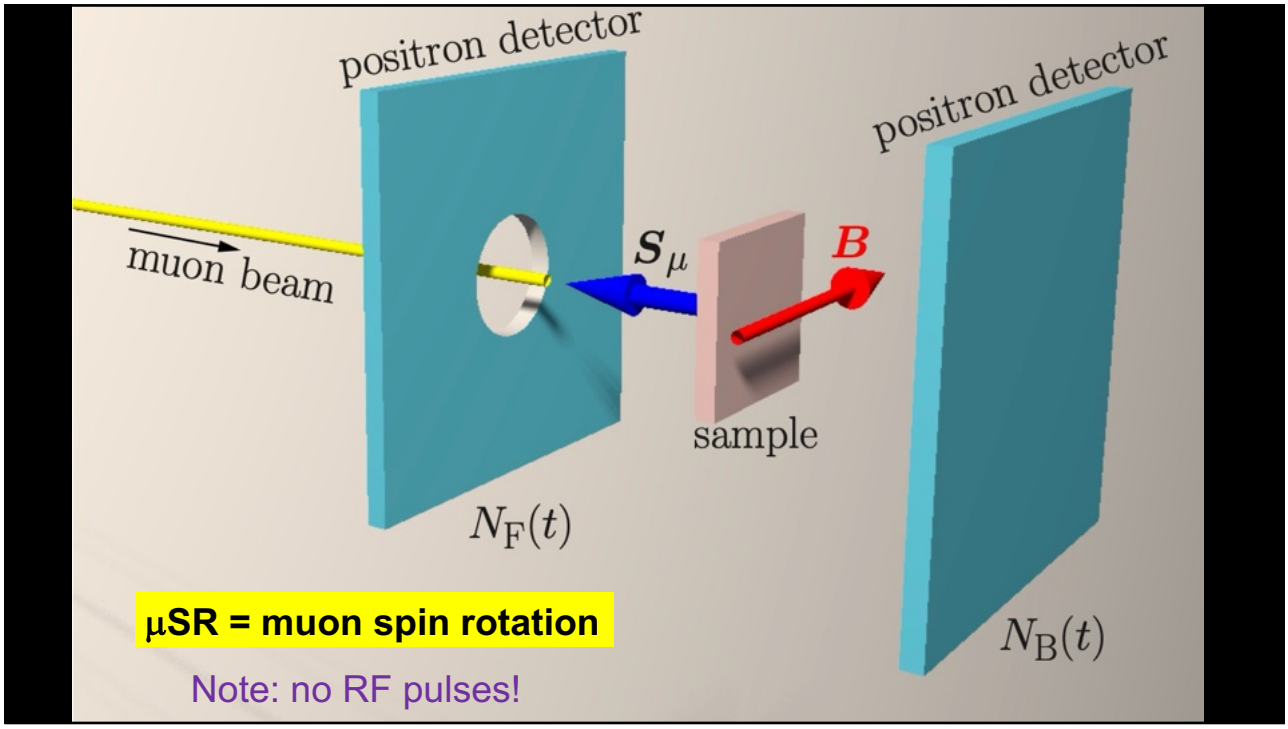
positron detector
positron detector
muon beam
S_μ
B
sample
$N_F(t)$
$N_B(t)$
μSR = muon spin rotation
Note: no RF pulses!

21

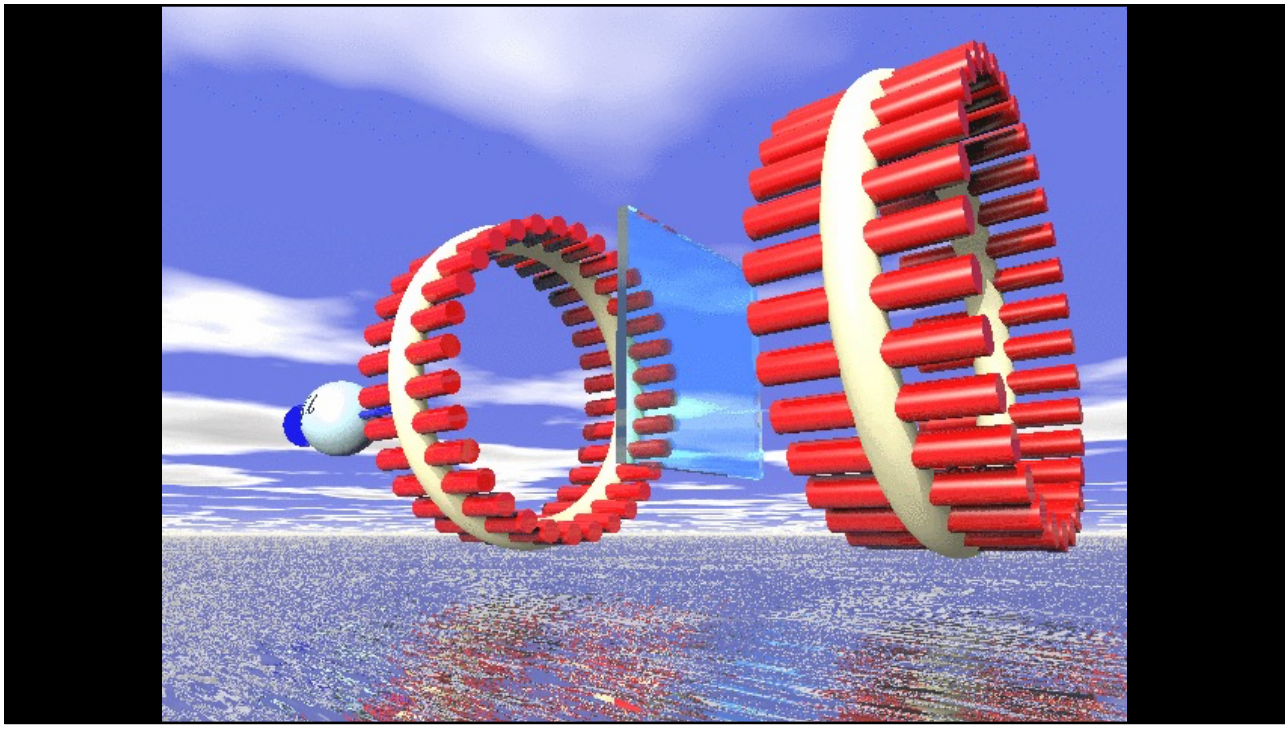

22

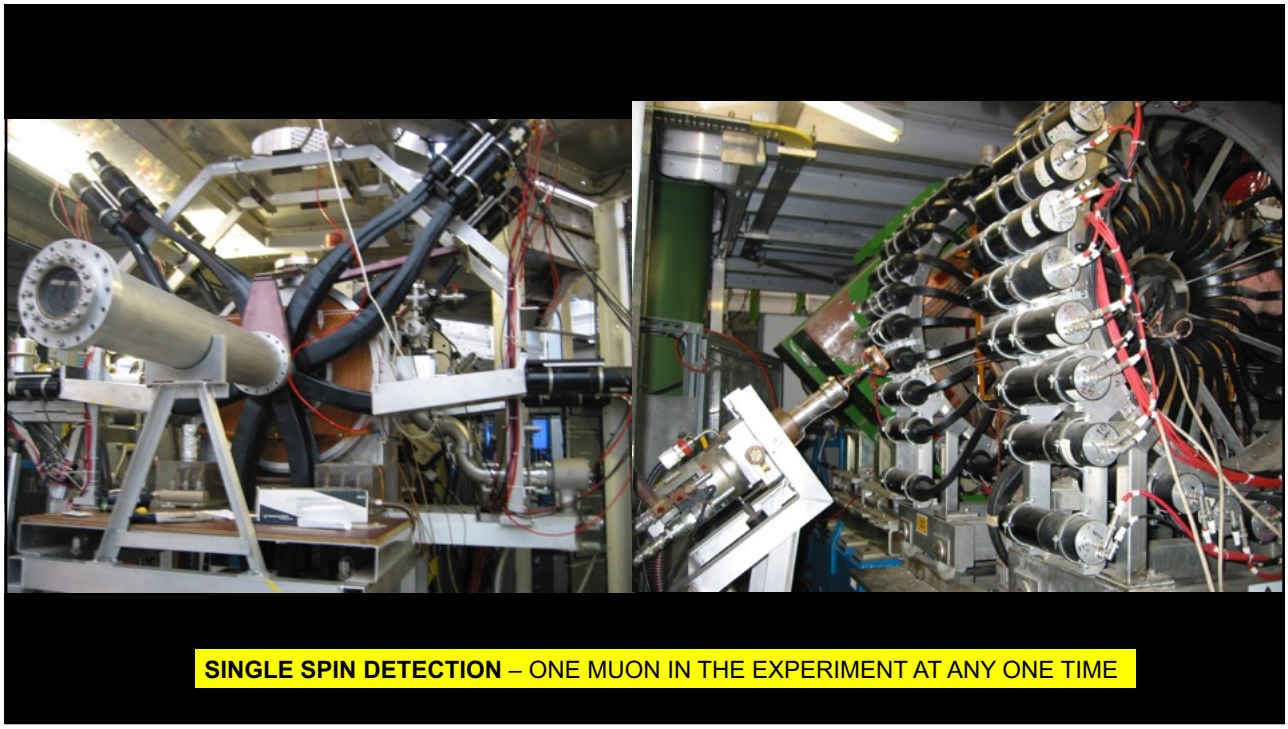
SINGLE SPIN DETECTION – ONE MUON IN THE EXPERIMENT AT ANY ONE TIME

23

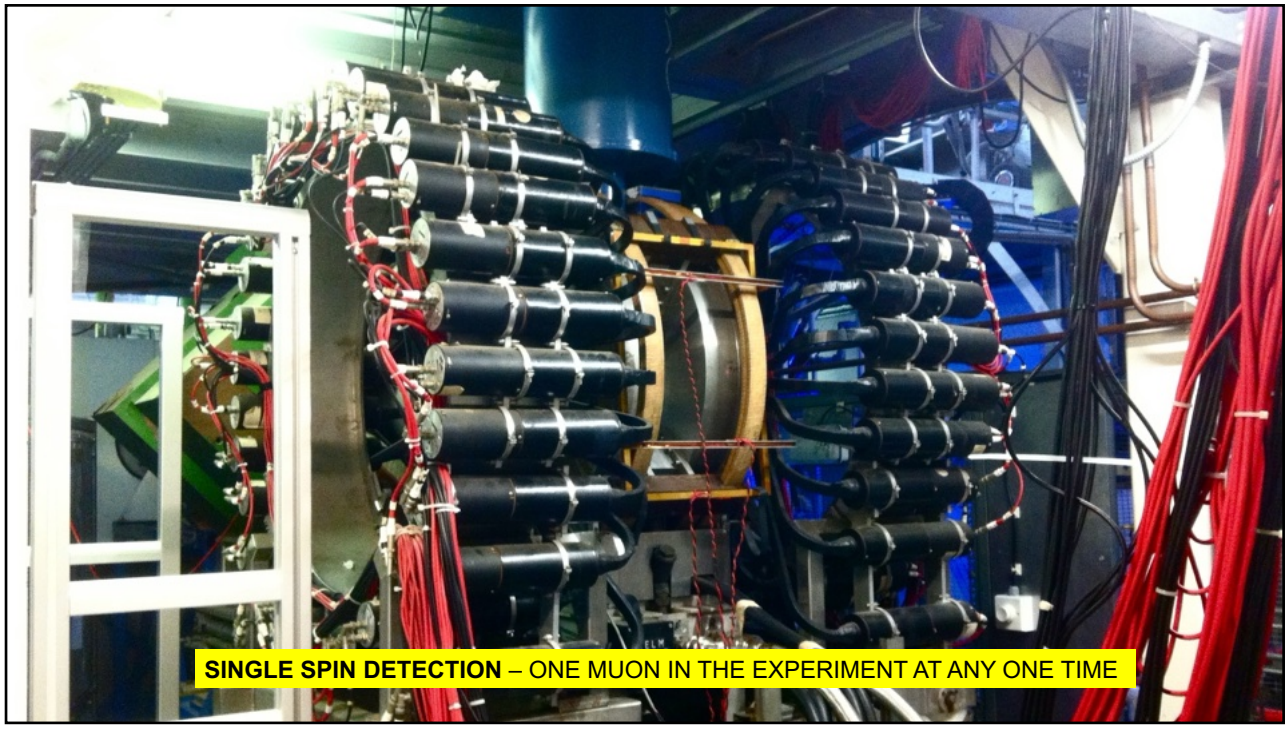
SINGLE SPIN DETECTION – ONE MUON IN THE EXPERIMENT AT ANY ONE TIME

24

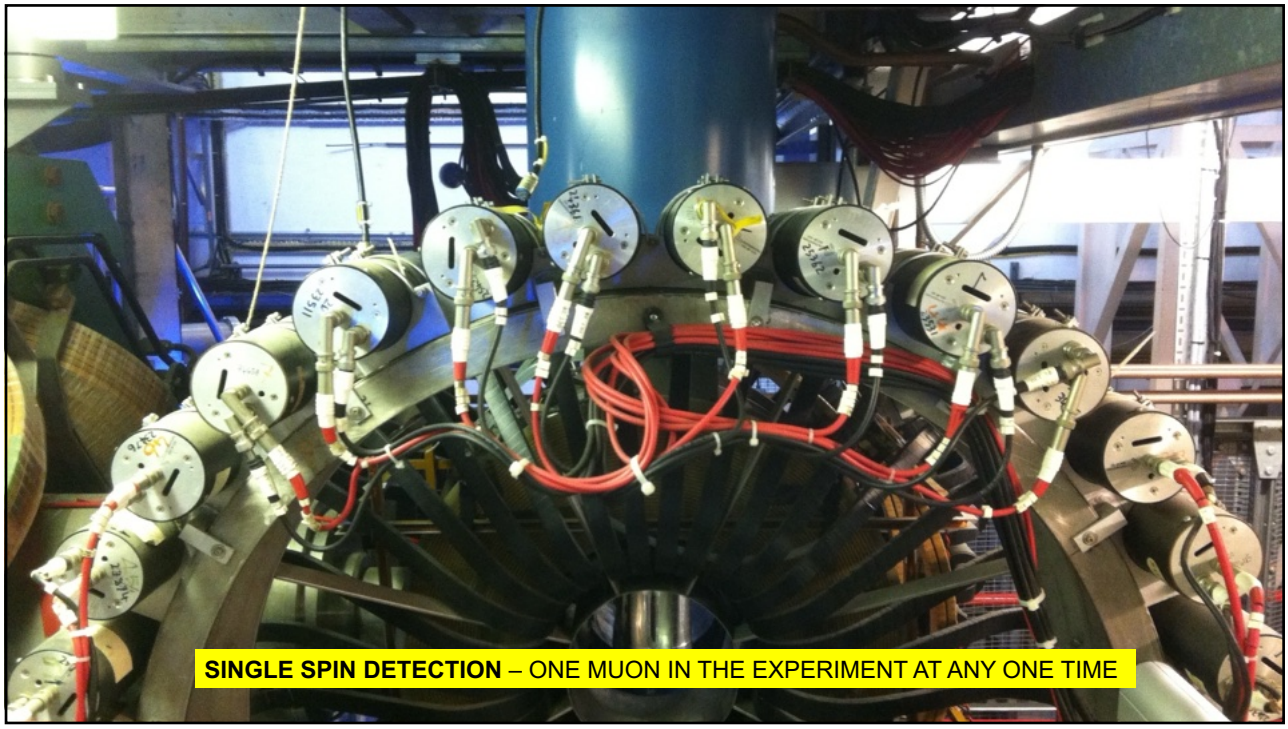
SINGLE SPIN DETECTION – ONE MUON IN THE EXPERIMENT AT ANY ONE TIME

25

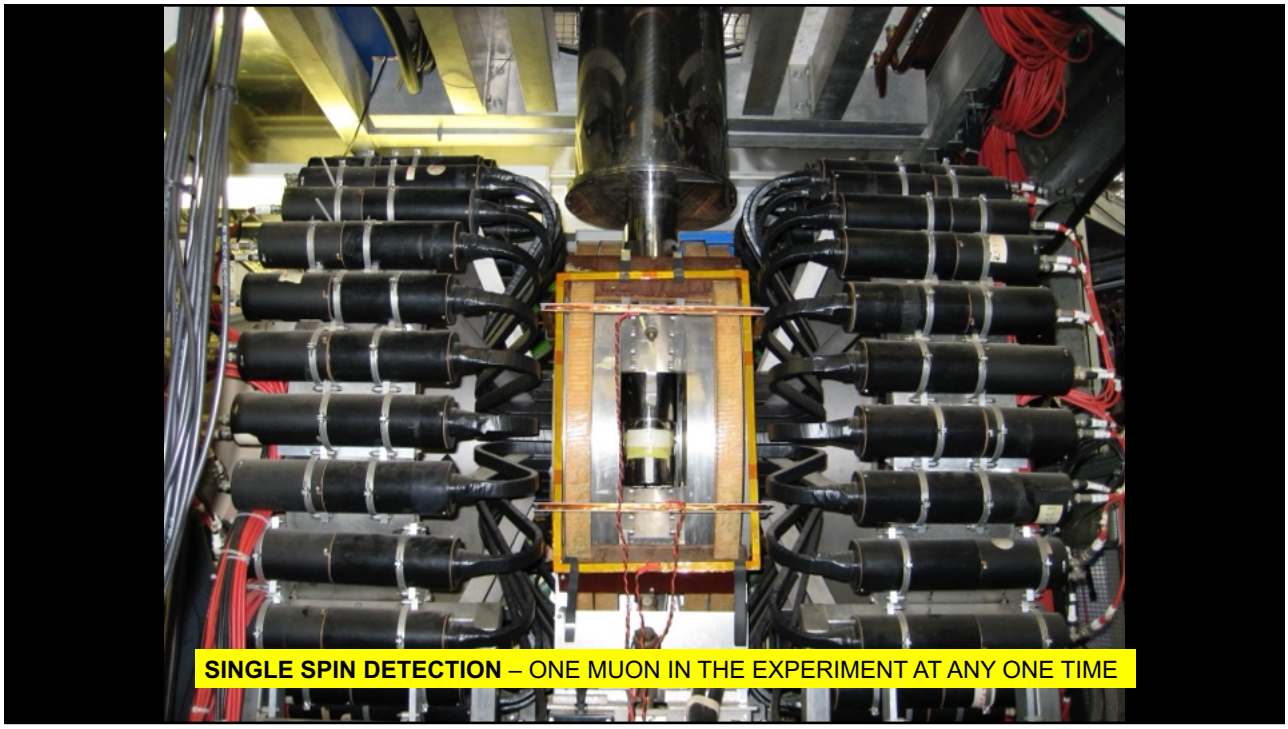
SINGLE SPIN DETECTION – ONE MUON IN THE EXPERIMENT AT ANY ONE TIME

26

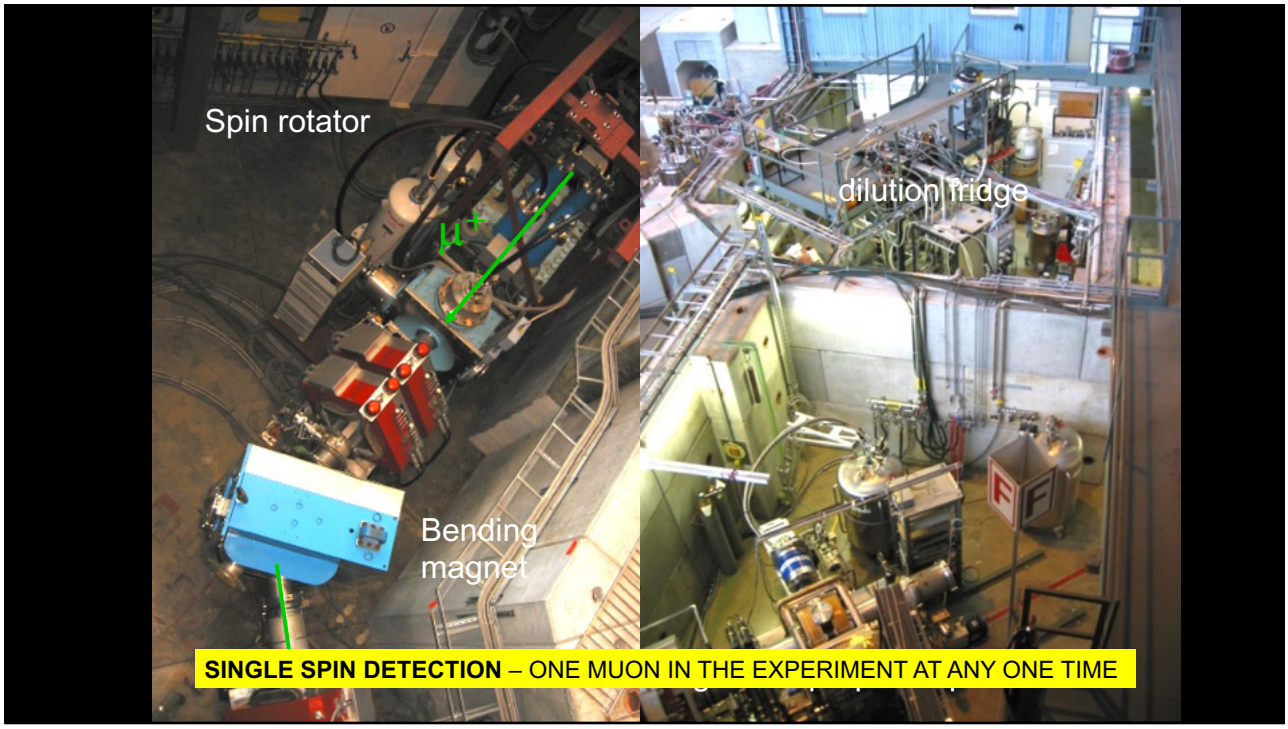
Spin rotator
μ^+
Bending magnet
dilution fridge
SINGLE SPIN DETECTION – ONE MUON IN THE EXPERIMENT AT ANY ONE TIME

27

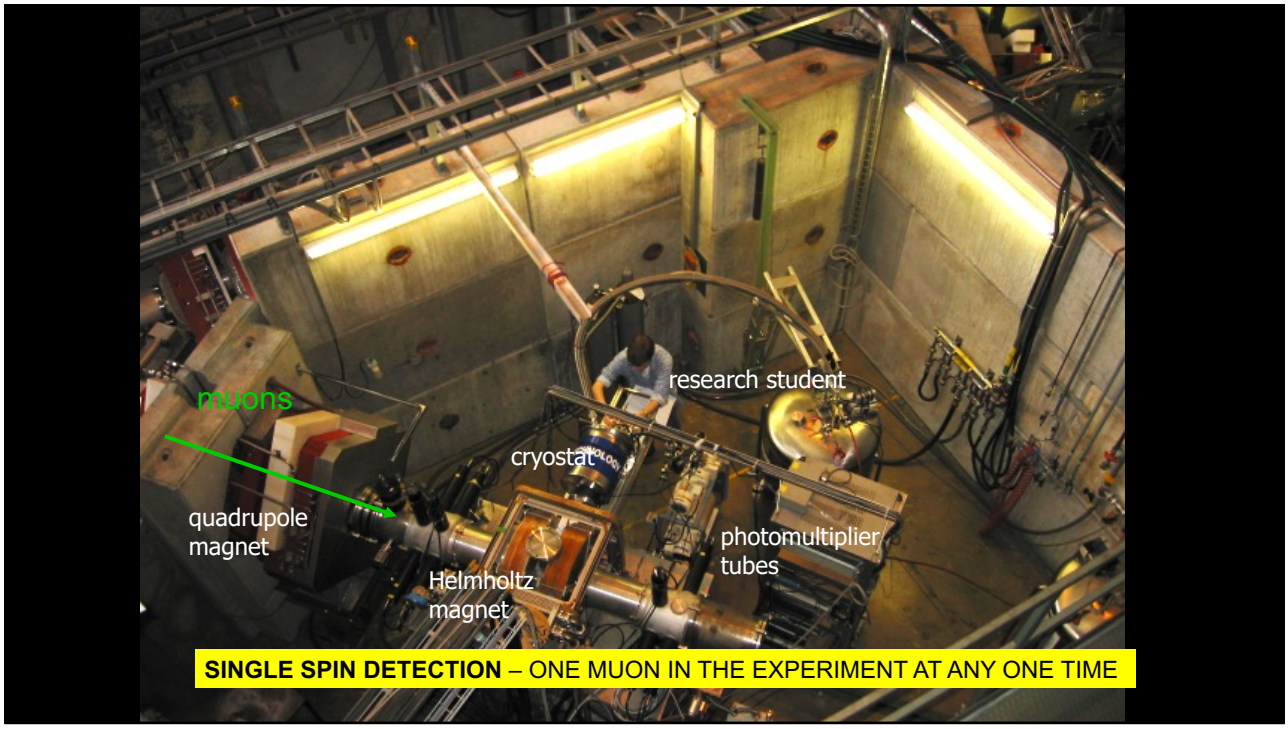
muons
research student
cryostat
quadrupole magnet
photomultiplier tubes
Helmholtz magnet
SINGLE SPIN DETECTION – ONE MUON IN THE EXPERIMENT AT ANY ONE TIME

28


SINGLE SPIN DETECTION – ONE MUON IN THE EXPERIMENT AT ANY ONE TIME

29

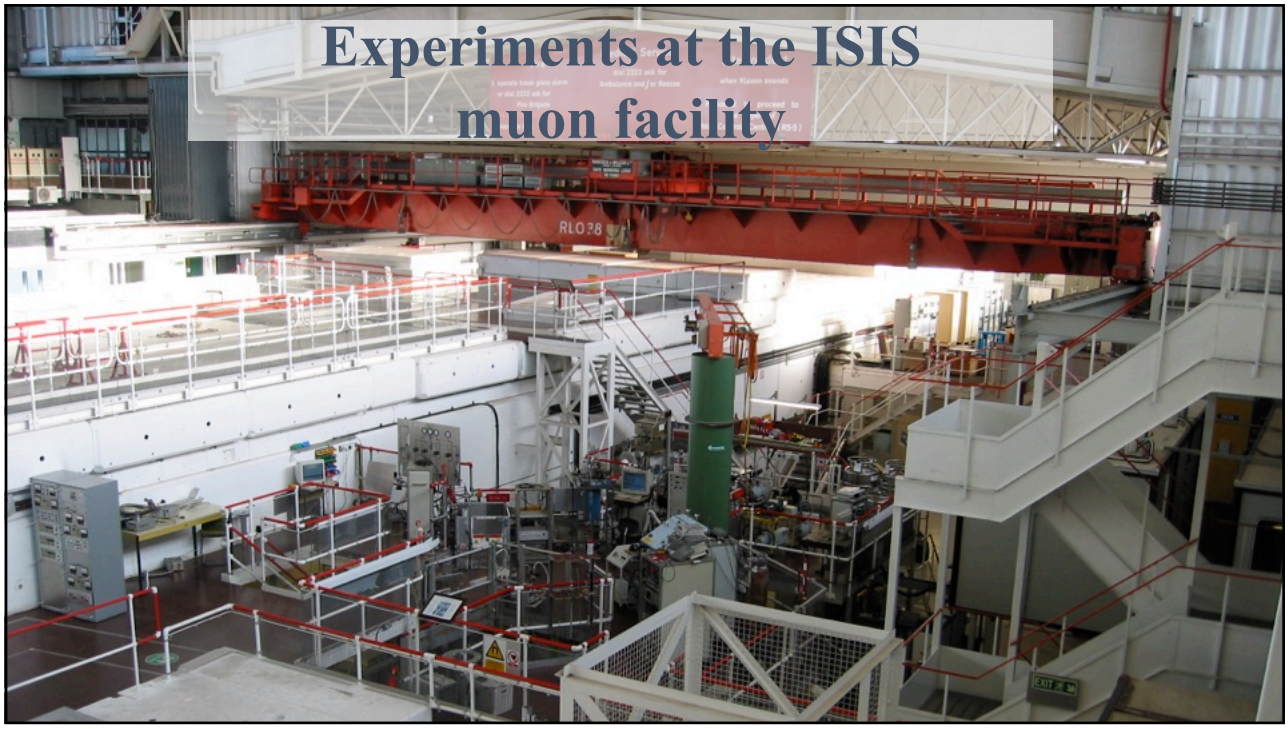
Experiments at the ISIS
muon facility

30

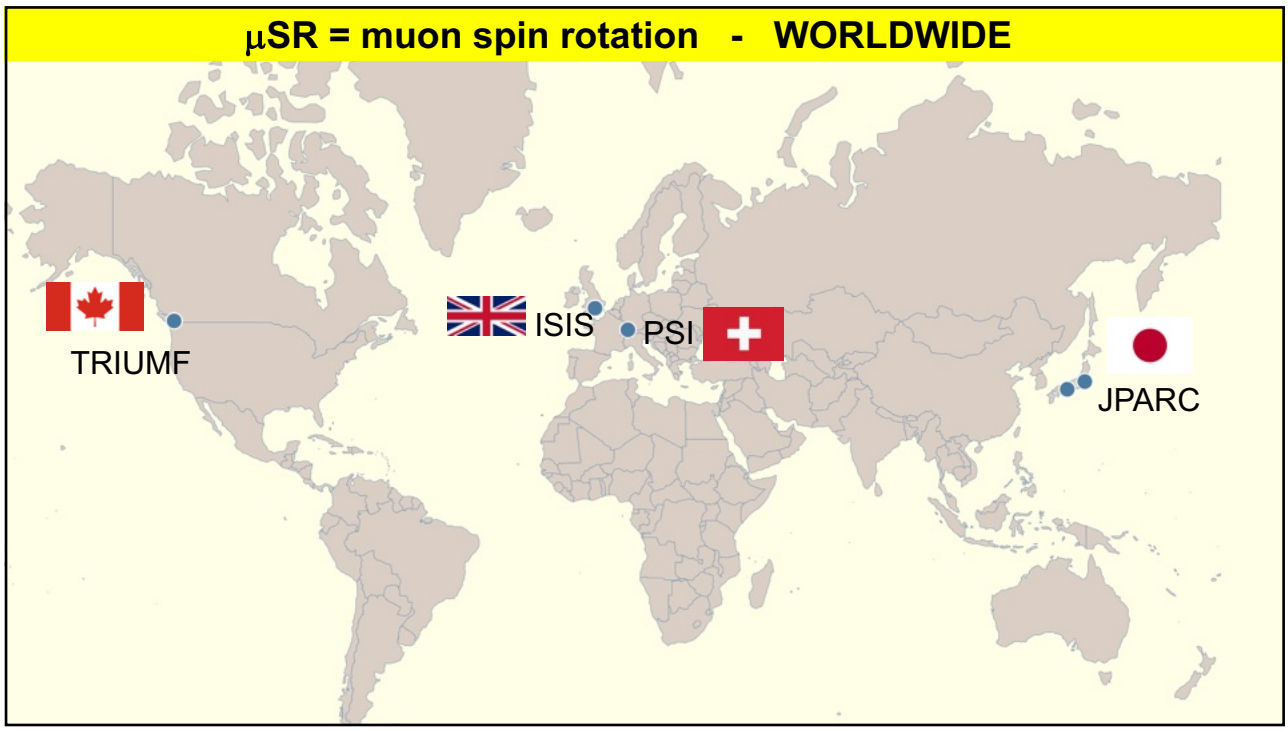
μSR = muon spin rotation - WORLDWIDE
TRIUMF
ISIS
PSI
JPARC

31

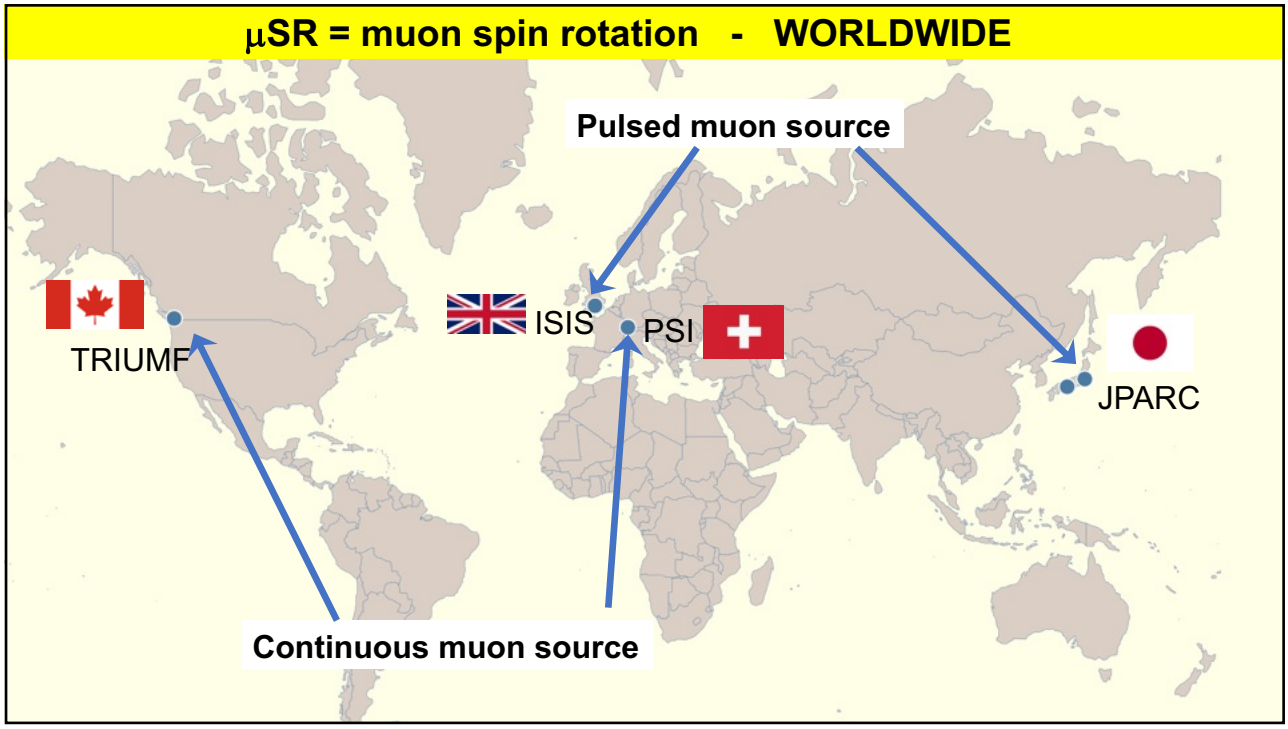
μSR = muon spin rotation - WORLDWIDE
Pulsed muon source
TRIUMF
ISIS
PSI
JPARC
Continuous muon source

32

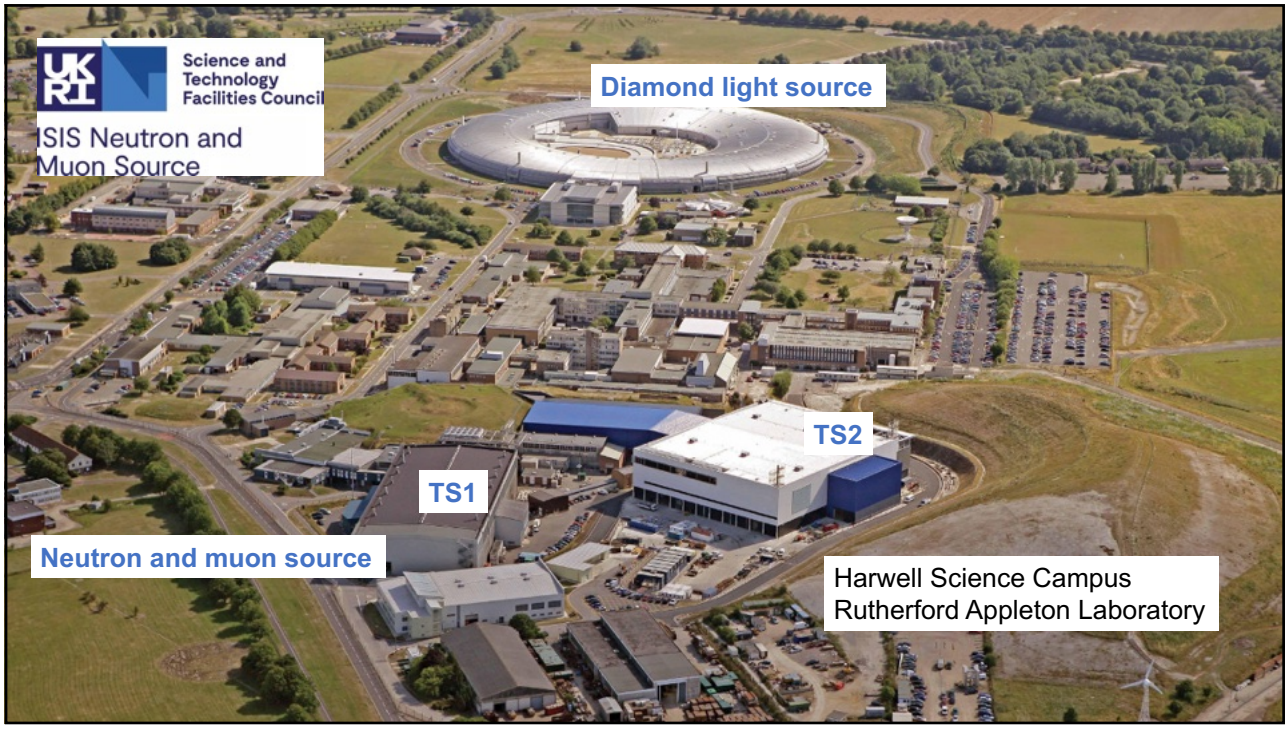
Science and Technology Facilities Council
ISIS Neutron and Muon Source
Diamond light source
TS2
TS1
Neutron and muon source
Harwell Science Campus
Rutherford Appleton Laboratory

33

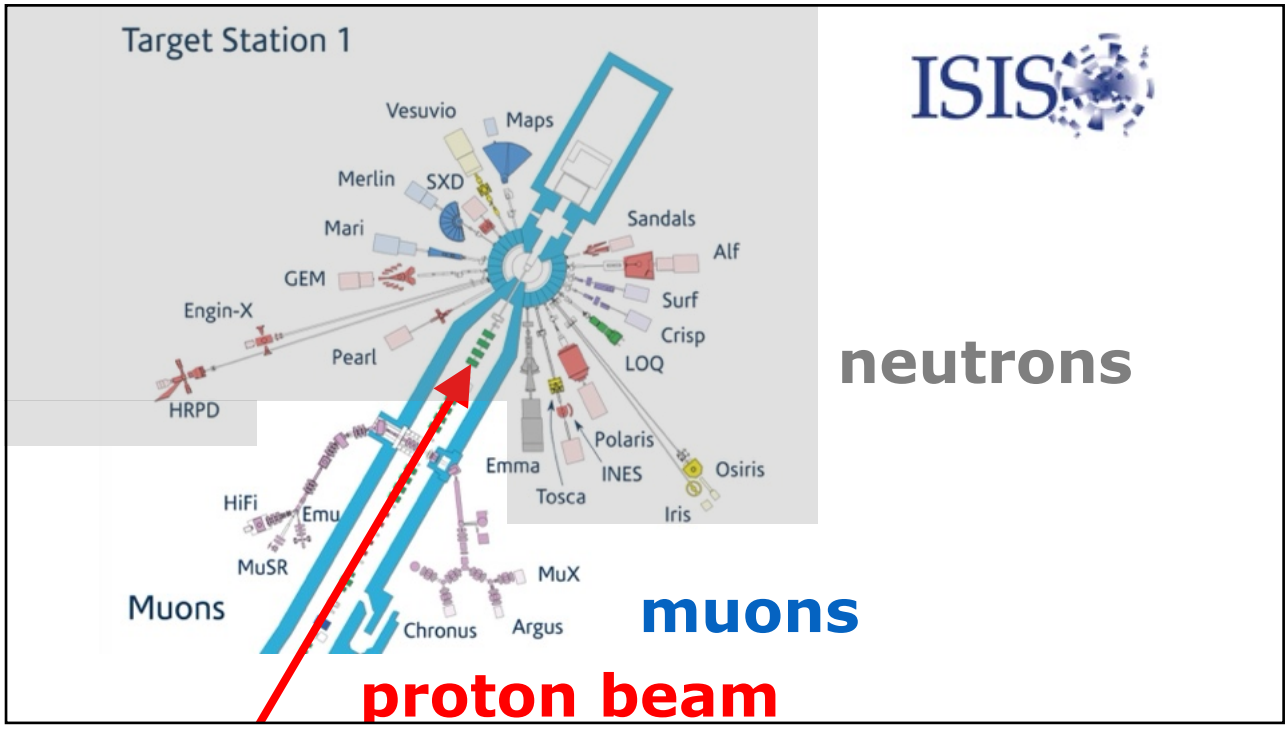
Target Station 1
ISIS
Vesuvio
Maps
Merlin
SXD
Mari
Sandals
Alf
GEM
Surf
Engin-X
Crisp
Pearl
LOQ
HRPD
Polaris
Emma
INES
Osiris
Tosca
Iris
HiFi
Emu
MuSR
MuX
Muons
Chronus
Argus
neutrons
muons
proton beam

34

μSR of purely organic magnets

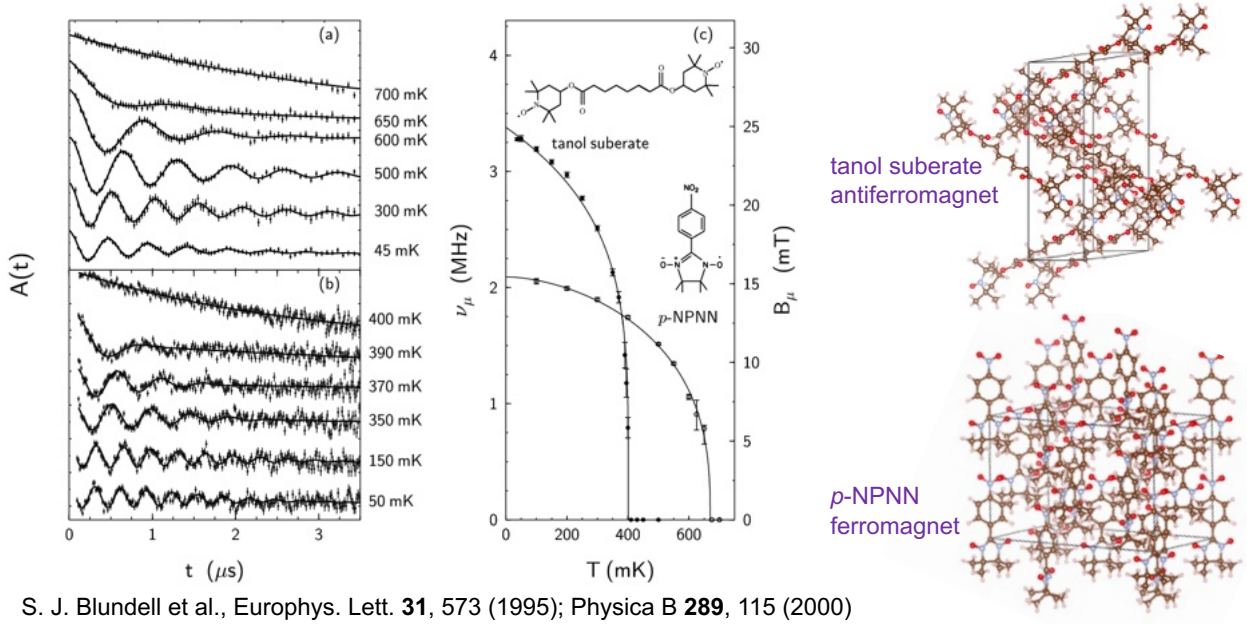

S. J. Blundell et al., Europhys. Lett. **31**, 573 (1995); Physica B **289**, 115 (2000)

35

μSR of purely organic magnets

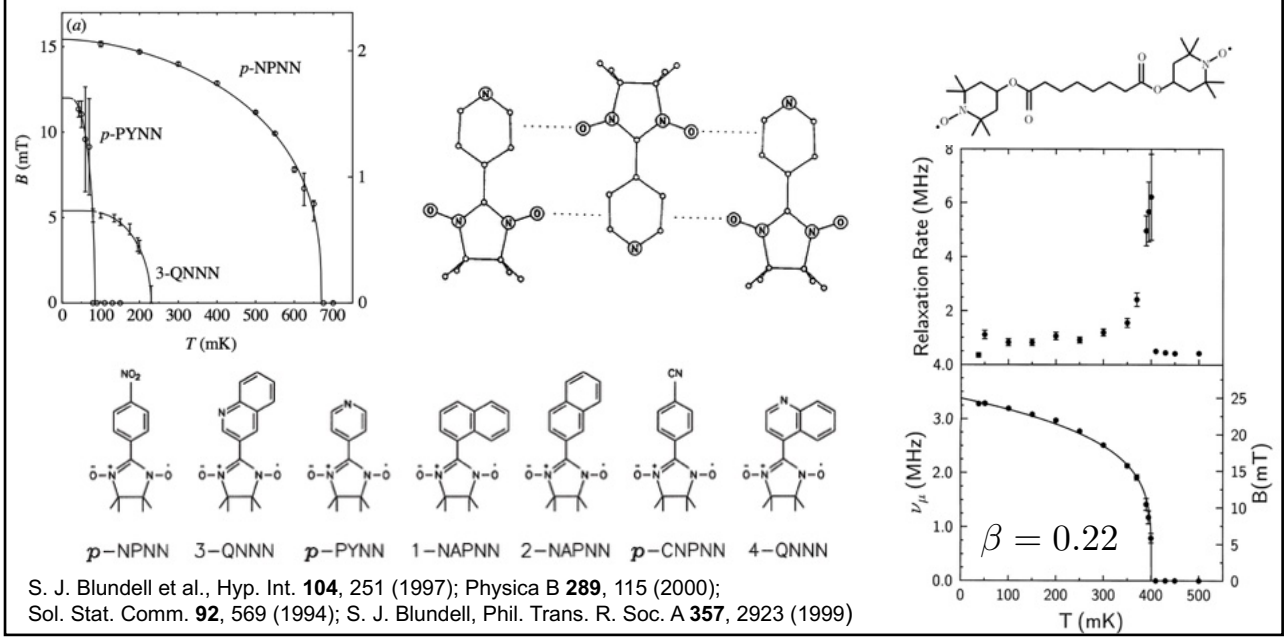

S. J. Blundell et al., Hyp. Int. **104**, 251 (1997); Physica B **289**, 115 (2000);
Sol. Stat. Comm. **92**, 569 (1994); S. J. Blundell, Phil. Trans. R. Soc. A **357**, 2923 (1999)

36

μSR of purely organic magnets

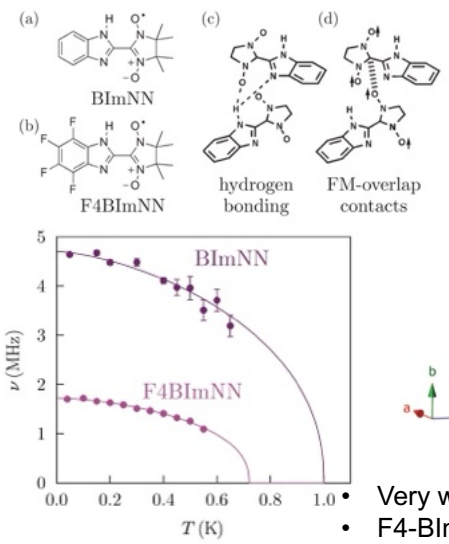

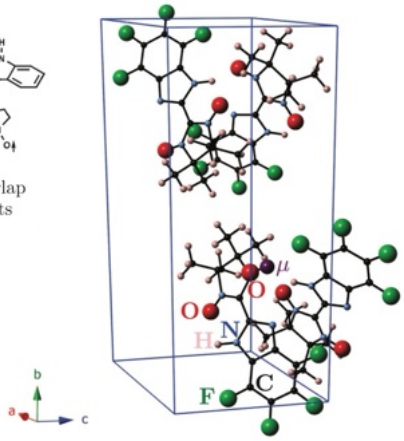

Compound	J/k_B (K)	T_c (K)	$k_B T_c/J$
γ phase *p*-NPNN	2.15	0.65	0.30
$Me_3NHCuCl_3 \cdot 2H$	0.85	0.165	0.19
$CuCl_2$(DMSO)	45	4.8	0.11
p-CDTV	6.0	0.67	0.11
$CuCl_2$(TMSO)	39	3	0.08
CHAC	45–53	2.18	0.04–0.05
p-CDpOV	5.5	0.21	0.038
TMCuC	30, 45	1.24	0.03–0.04
CHAB	55	1.50	0.027
BImNN	22	1.0	0.045
F4BImNN	22	0.72	0.033

$$\mathcal{H} = -J \sum_{\langle i,j \rangle} \mathbf{S}_i \cdot \mathbf{S}_j - J' \sum_{\langle i,i' \rangle} \mathbf{S}_i \cdot \mathbf{S}_{i'},$$

- Very well-defined one-dimensional ferromagnetism due to small $k_B T_c/J$
- F4-BImNN is the best realized purely organic 1d Heinsenberg ferromagnet

T. Sugano, S. J. Blundell, T. Lancaster, F. L. Pratt, and H. Mori, Phys. Rev. B **82**, 180401(R) (2010)
S. J. Blundell, J. S. Möller, T. Lancaster, P. J. Baker, F. L. Pratt, G. Seber and P. M. Lahti, Phys. Rev. B **88**, 064423 (2013)

37

spin-1/2 chain: $Cu(NO_3)_2$(pyrazine)

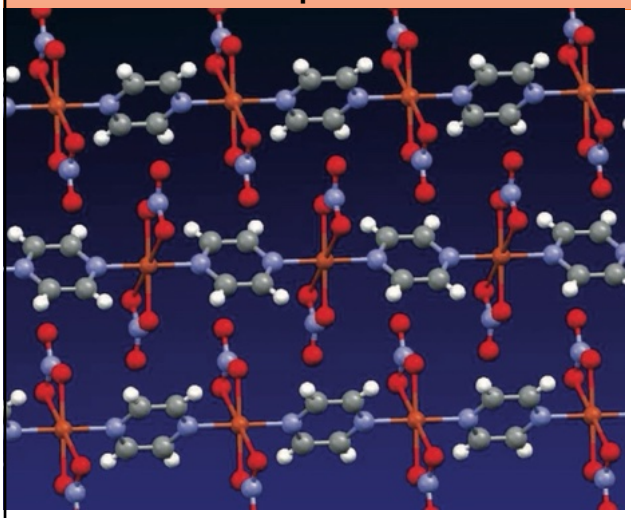

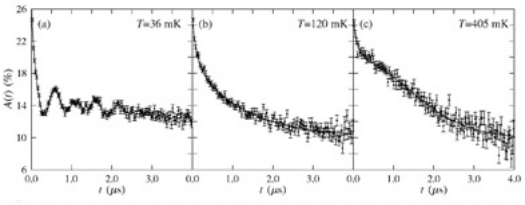

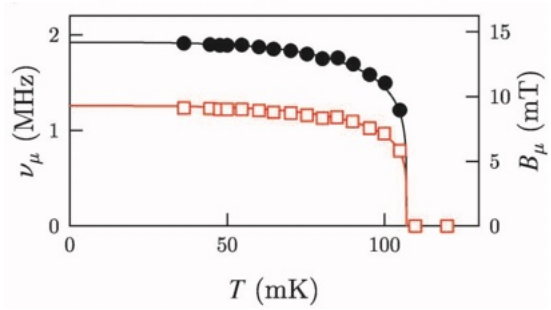

$J/k_B \approx 10.3\,\mathrm{K}$ $T_N = 107$ mK $k_B T_N/J \approx 0.01$

T. Lancaster, S. J. Blundell, M. L. Brooks, P. J. Baker, F. L. Pratt, J. L. Manson, C. P. Landee and C. Baines, Phys. Rev. B **73**, R020410 (2006)

38

Heat capacity versus μSR

Magnetic heat capacity

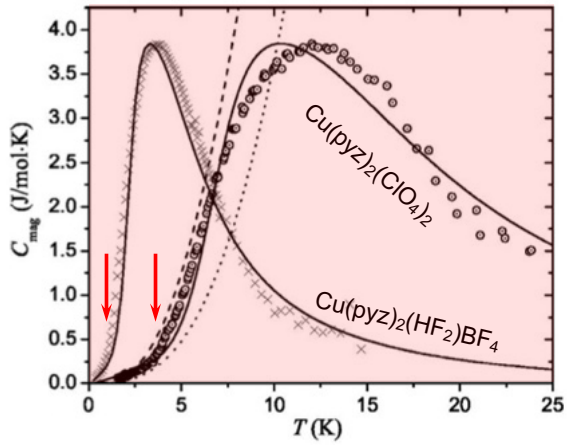

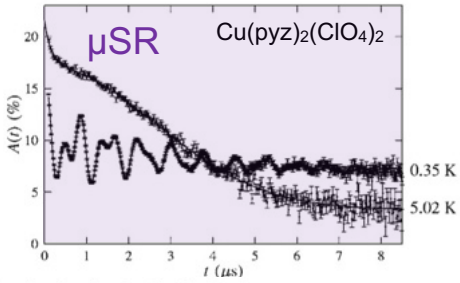

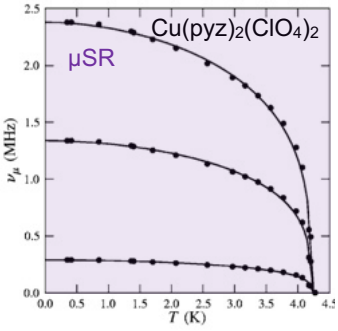

Cu(pyz)2(HF2)BF4

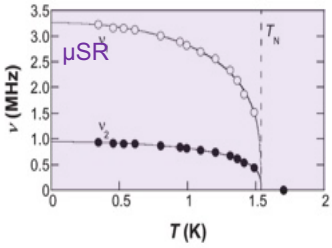

J. L. Manson et al. Chem. Comm. 4894 (2006); T. Lancaster et al. Phys. Rev. B **75**, 094421 (2007)

39

Magnetic susceptibility versus μSR

Cu(HCO2)(NO3)(pyz)

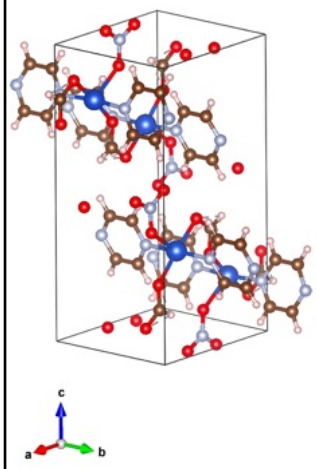

Magnetic susceptibility

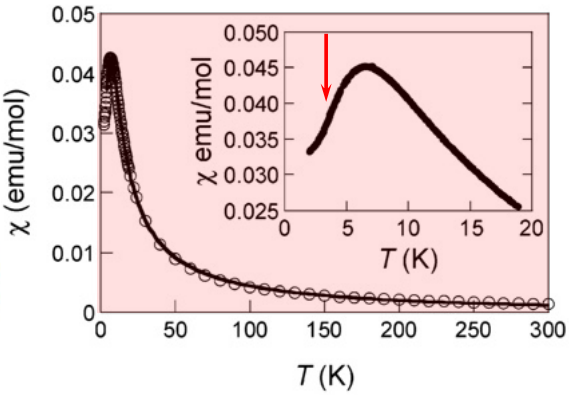

μSR

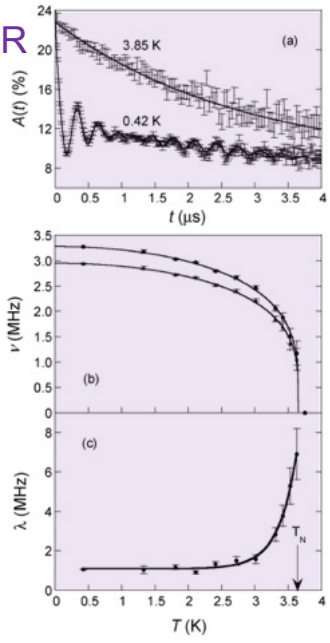

J. L. Manson, T. Lancaster, J. A. Schlueter, S. J. Blundell, M. L. Brooks, F. L. Pratt, C. L. Nygren, H. J. Koo, D. Dai and M. H. Whangbo, Inorg. Chem. **46**, 213 (2007)

40

μSR: ν(*T*) for many low-dimensional molecular magnets

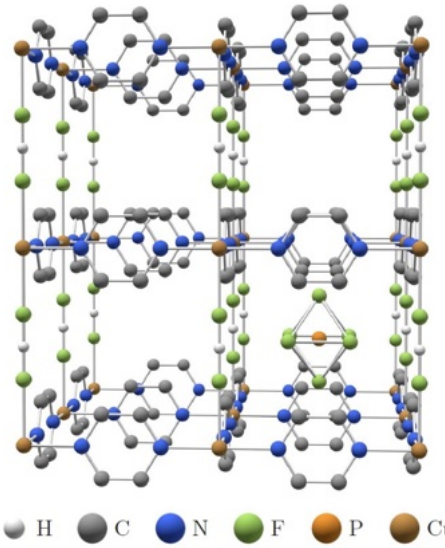

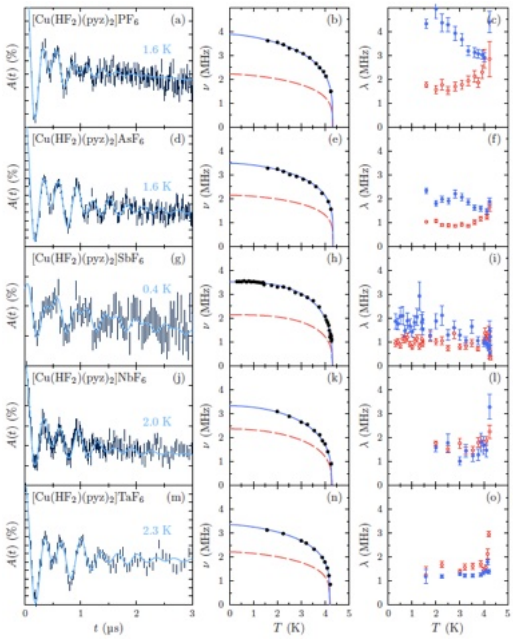

A.J. Steele, T. Lancaster, S. J. Blundell, P. J. Baker, F. L. Pratt, C. Baines, M. M. Conner, H. I. Southerland, J. L. Manson and J. A. Schlueter, Phys. Rev. B **84**, 064412 (2011)

41

Highly isolated spin-1/2 chain: DEOCC-$TCNQF_4$

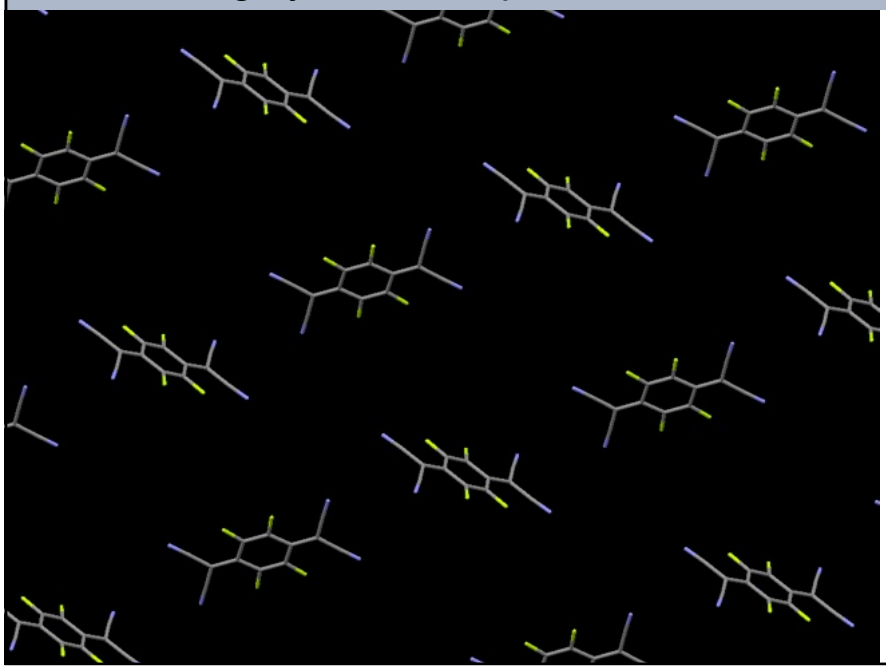

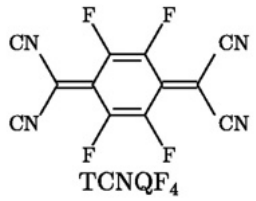

42

Highly isolated spin-1/2 chain: DEOCC-TCNQF$_4$

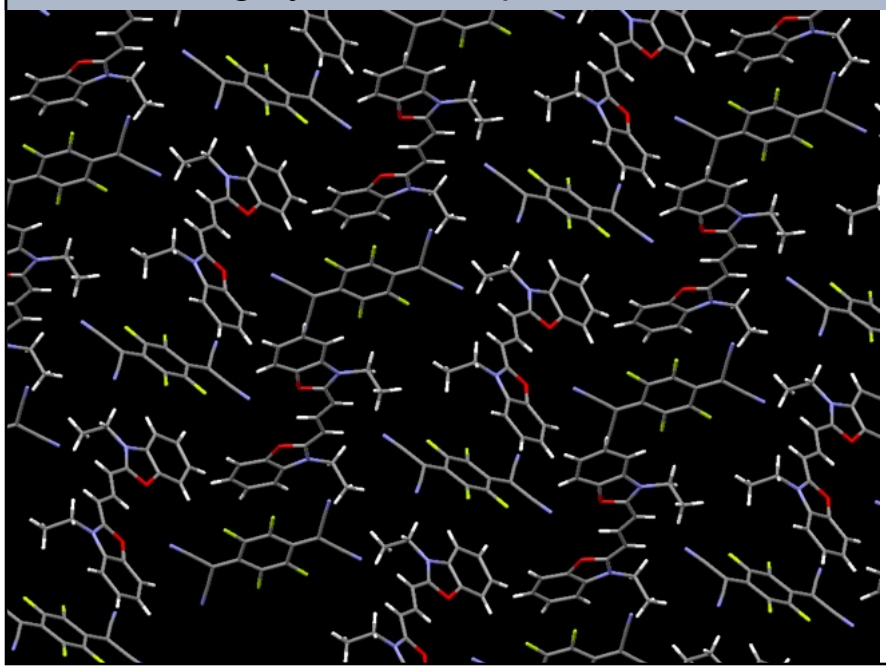

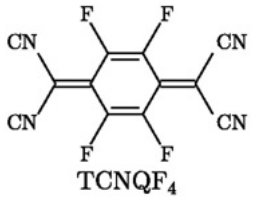

TCNQF$_4$

DEOCC$^+$

43

Highly isolated spin-1/2 chain: DEOCC-TCNQF$_4$

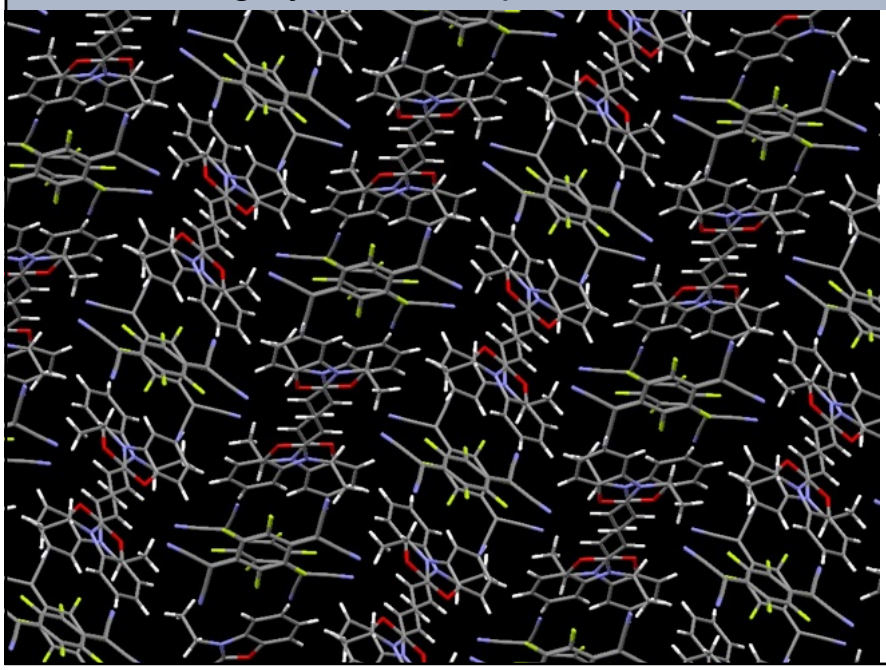

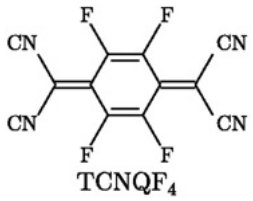

TCNQF$_4$

DEOCC$^+$

44

Highly isolated spin-1/2 chain: DEOCC-TCNQF$_4$

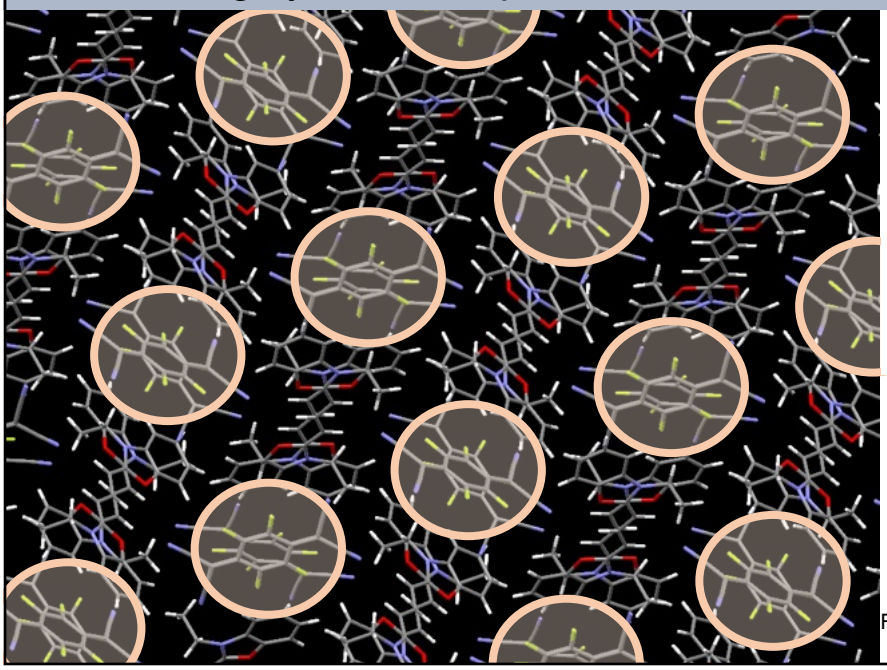

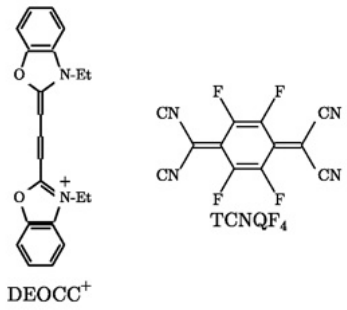

$$J = 110\,\mathrm{K}$$

$$T_\mathrm{N}/J < 0.00018$$

F. L. Pratt et al. PRL **96,** 247203 (2006)

45

Highly isolated spin-1/2 2d Heisenberg: Ag(pyz)$_2$(S$_2$O$_8$)

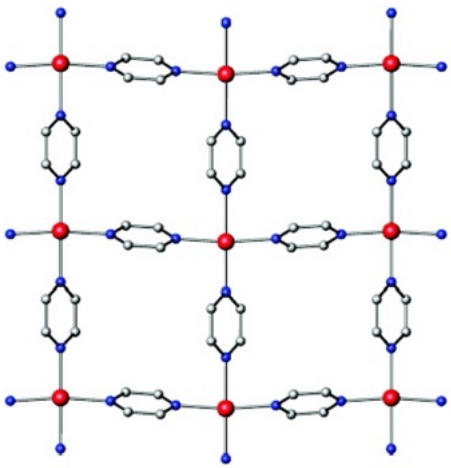

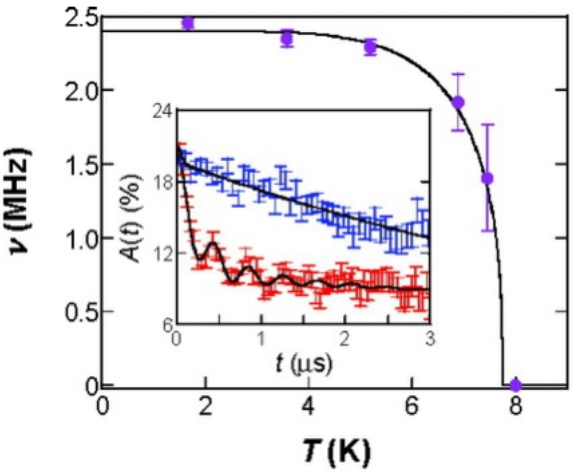

$$J \approx 53\,\mathrm{K}$$

$$T_\mathrm{N} = 7.8(3)\ \mathrm{K}$$

J. L. Manson et al. J. Am. Chem. Soc. **131,** 4590 (2009)

46

Relationship between T_N/J and J'/J in 1d and 2d

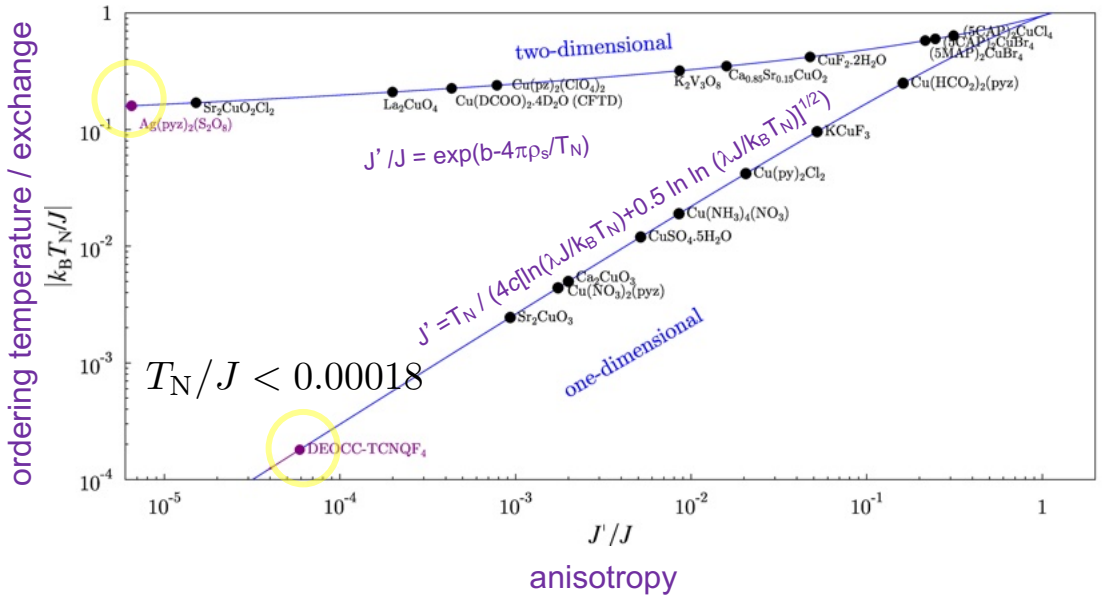

S. J. Blundell et al., J. Phys. Chem. Solids **68**, 2039 (2007)

47

Muons and superconductors

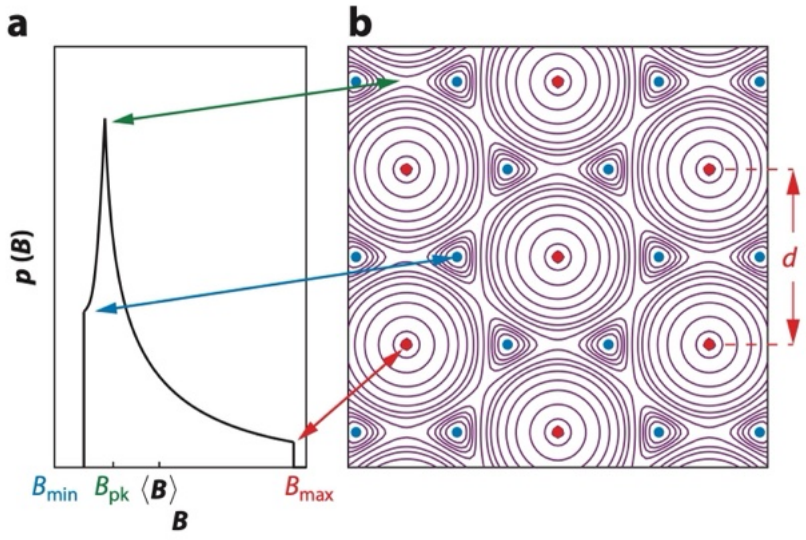

Figure from: S. J. Blundell, Ann. Rev. Condens. Matter Phys. **16**, 367 (2025)

48

NaFeAs

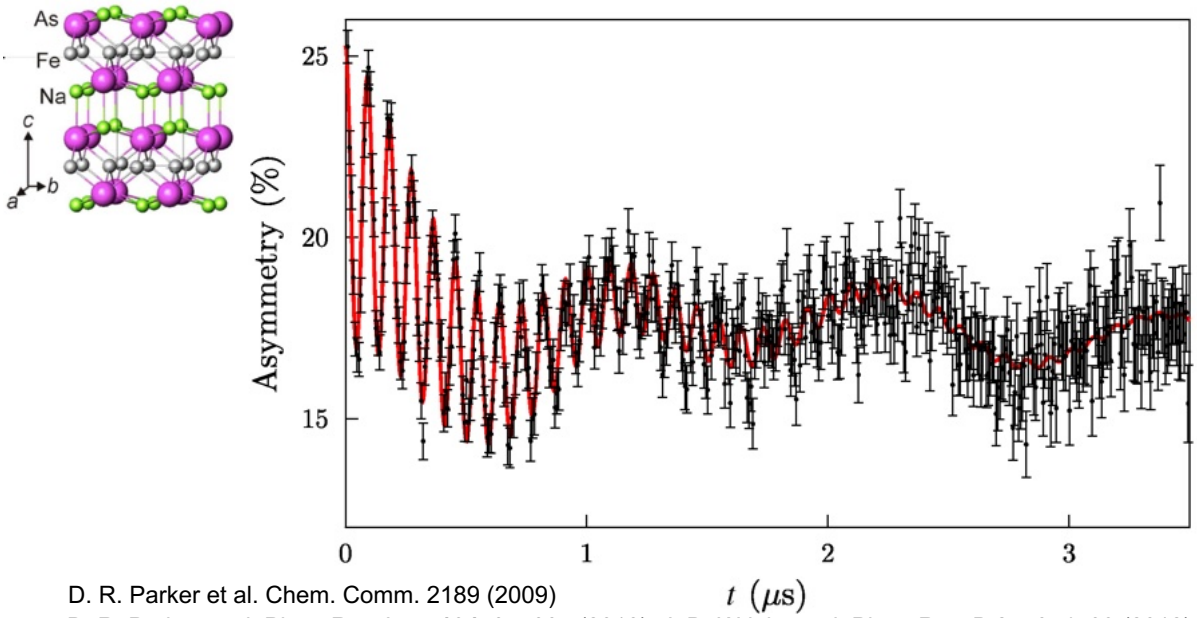

D. R. Parker et al. Chem. Comm. 2189 (2009)
D. R. Parker et al. Phys. Rev. Lett. **104**, 057007 (2010); J. D. Wright et al. Phys. Rev. B **85**, 054503 (2012)

49

$NaFe_{1-x}Co_xAs$

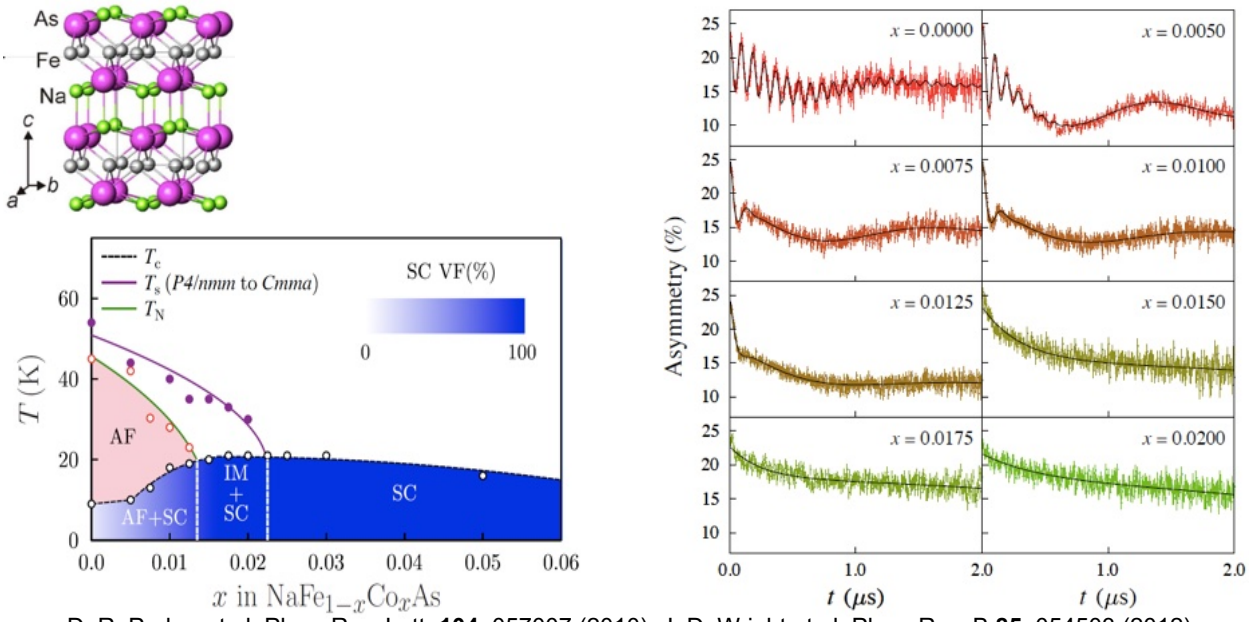

D. R. Parker et al. Phys. Rev. Lett. **104**, 057007 (2010); J. D. Wright et al. Phys. Rev. B **85**, 054503 (2012)

50

$NaFe_{1-x}Co_xAs$

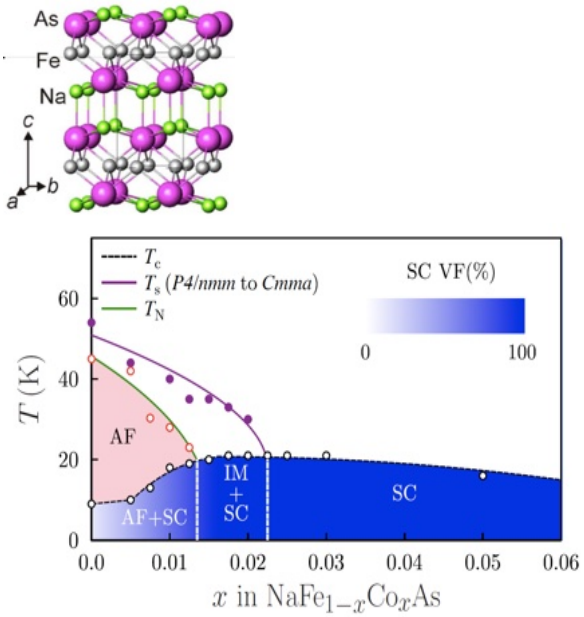

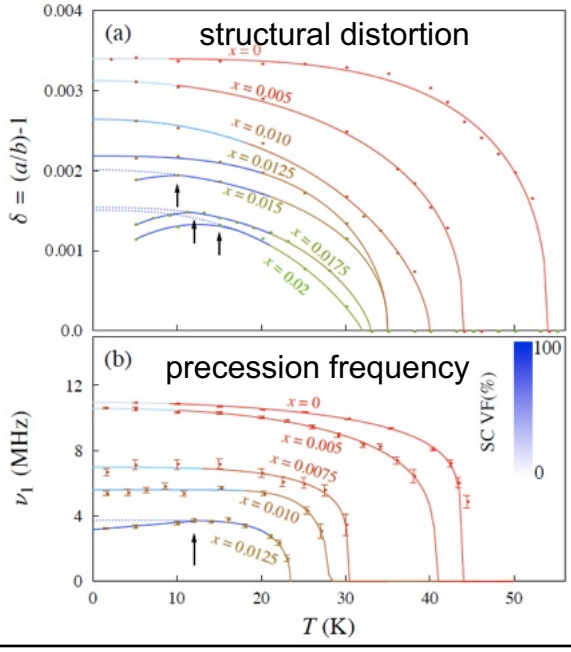

J. D. Wright et al. Phys. Rev. B **85**, 054503 (2012)

51

Molecular intercalation of FeSe

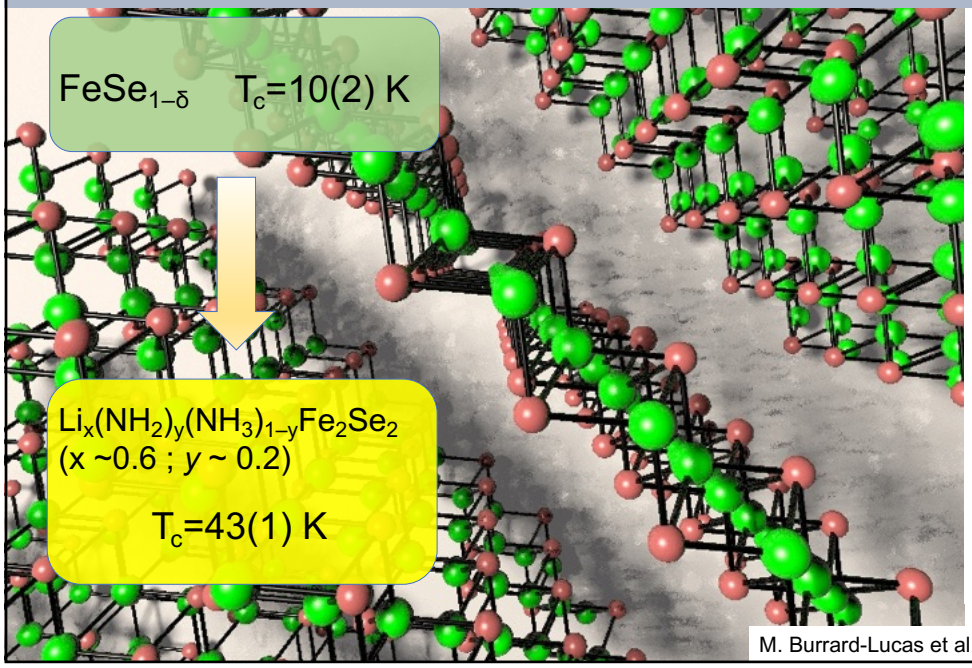

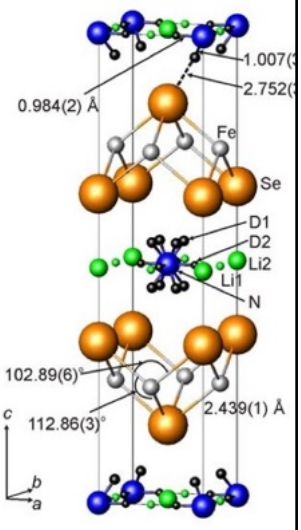

M. Burrard-Lucas et al. Nature Materials **12**, 15 (2013)

52

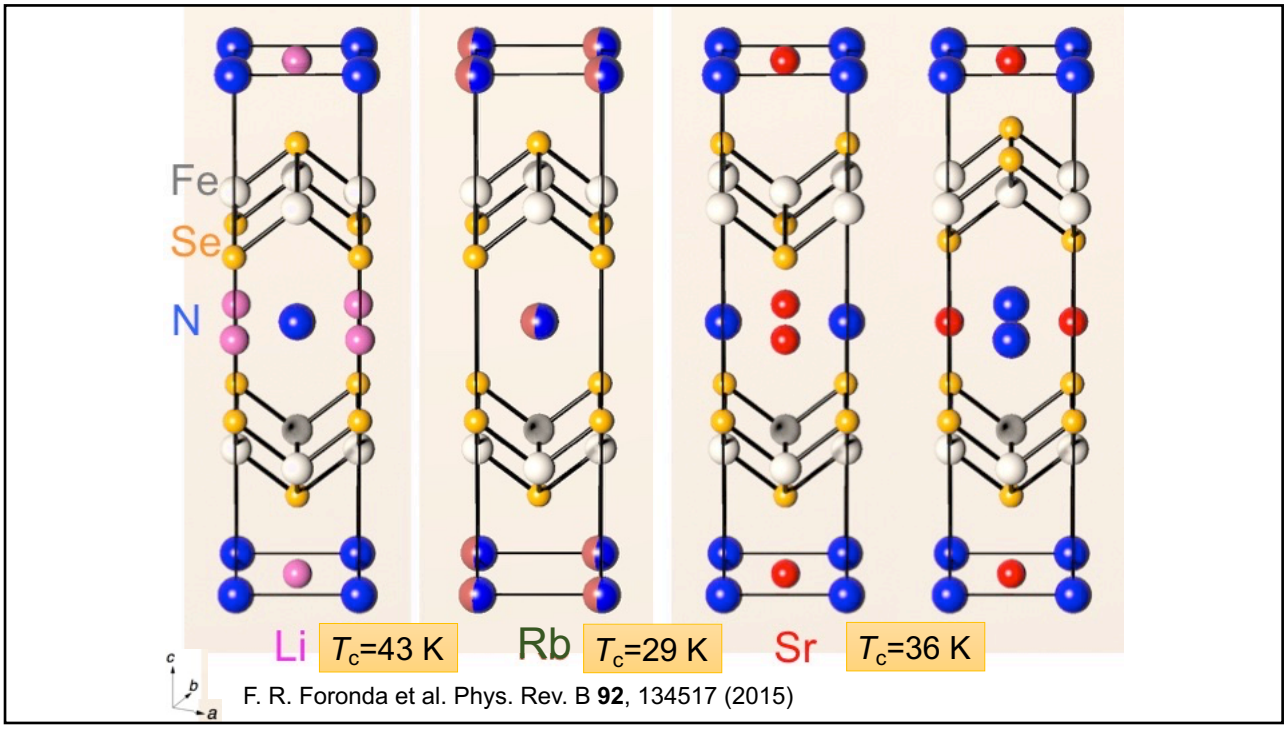

F. R. Foronda et al. Phys. Rev. B **92**, 134517 (2015)

53

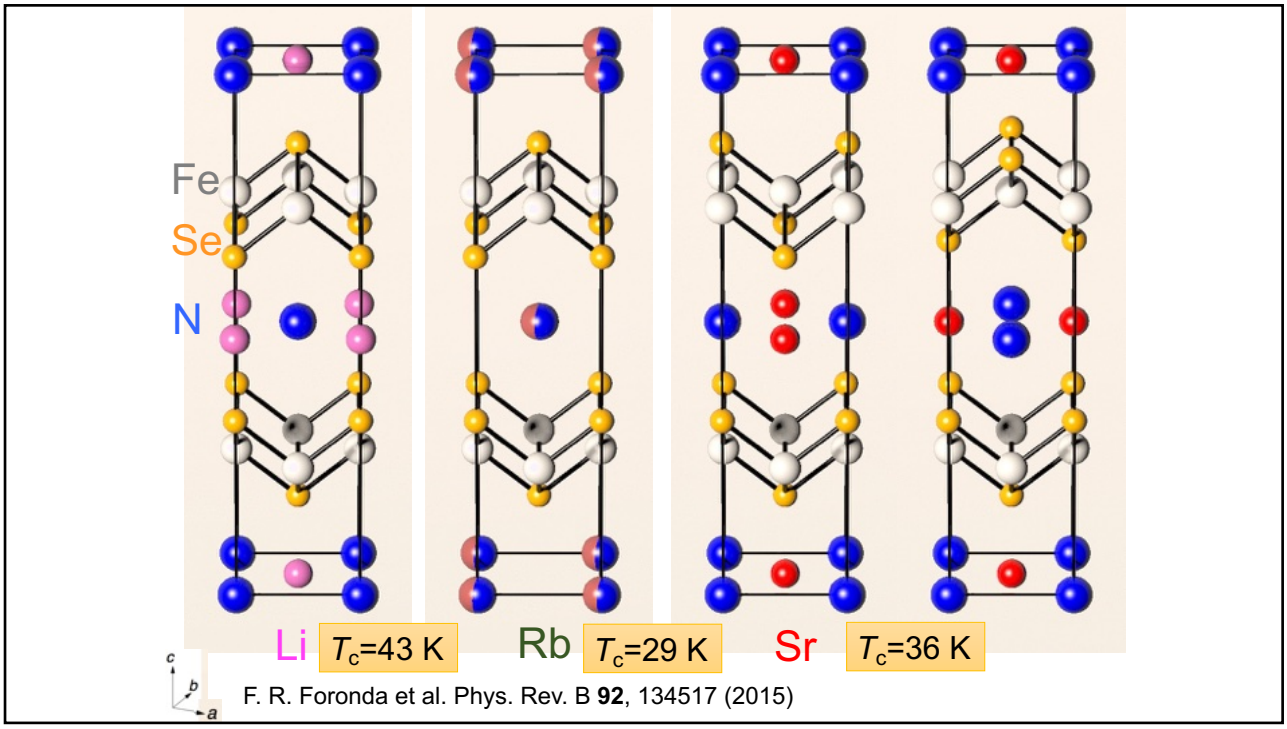

F. R. Foronda et al. Phys. Rev. B **92**, 134517 (2015)

54

Uemura plot of some iron-based superconductors

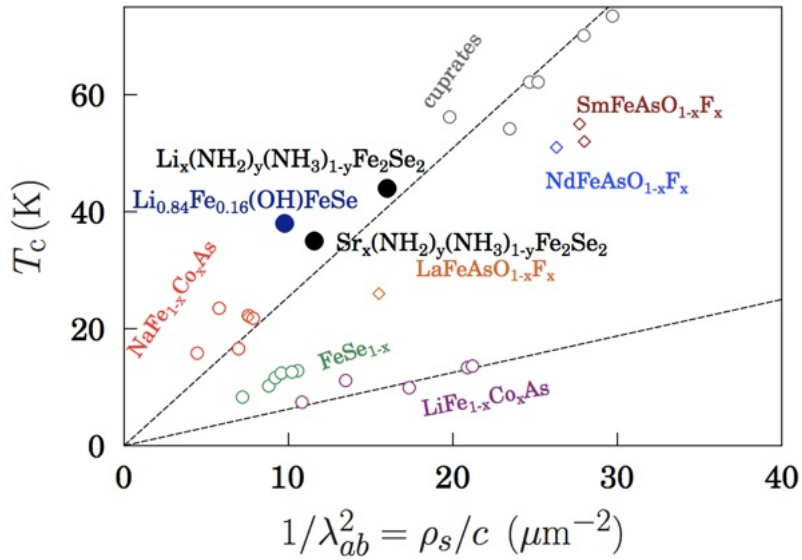

M. Burrard-Lucas et al. Nature Materials **12**, 15 (2013); H. Sun, et al. Inorg. Chem. **54**, 1958 (2015); F. R. Foronda et al., Phys. Rev. B **92**, 134517 (2015); F. L. Pratt et al. Phys. Rev. B **79**, 052508 (2009); M. J. Pitcher et al. JACS **132**, 10467 (2010); D. R. Parker et al. Phys. Rev. Lett. **104**, 057007 (2010)

55

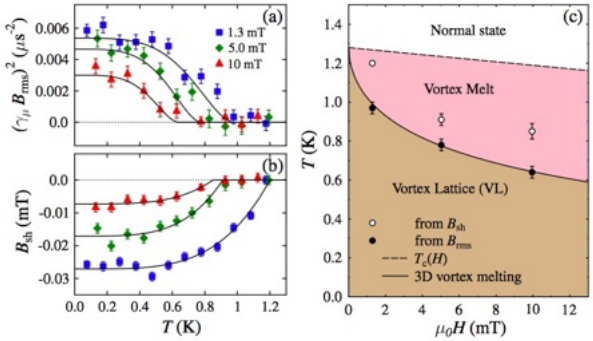

Low field phase of the molecular superconductor $(TMTSF)_2ClO_4$

F. L. Pratt, T. Lancaster, S. J. Blundell and C. Baines, Phys. Rev. Lett. **110**, 107005 (2013)

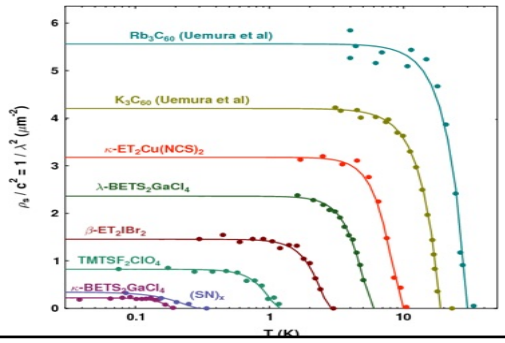

ρ_s across the range of molecular superconductors

F. L. Pratt and S. J. Blundell, Phys. Rev. Lett. **94**, 097006 (2005)

56

Coexistence of superconductivity and magnetism by chemical design and nanosheet assembly

superconducting
TaS_2

magnetic
$M(OH)_2$

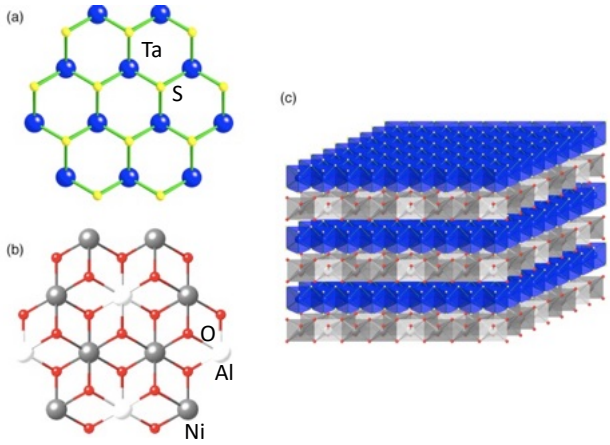

$[Ni_{0.66}Fe_{0.33}(OH)_2][TaS_2]$ T_c (super) ~ 4 K T_N (magnetic) ~ 16 K

E. Coronado, C. Marti-Gastaldo, E. Navarro-Moratalla, A. Ribera, S. J. Blundell and P. J. Baker, Nature Chemistry **2**, 1031 (2010)

57

Tuning the interlayer spacing in high T_c superconductors

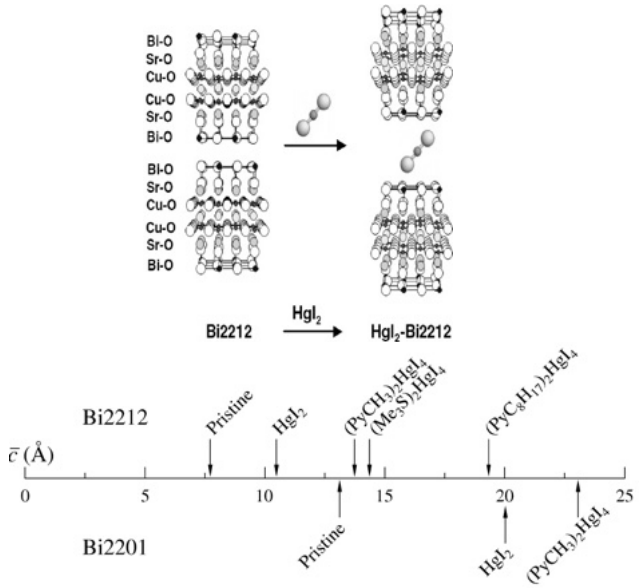

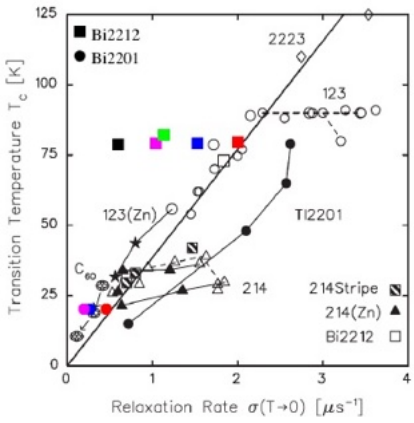

$$\rho_s \propto \lambda^{-2} \propto \frac{1}{d}$$

P.J. Baker, T. Lancaster, S. J. Blundell, F.L. Pratt, M.L. Brooks and S.-J. Kwon, Phys. Rev. Lett. 102, 087002 (2009); J.-H. Choy, S. J. Kwon, and K. S. Park, Science 280, 1589 (1998).

58

Muon data on molecular magnets

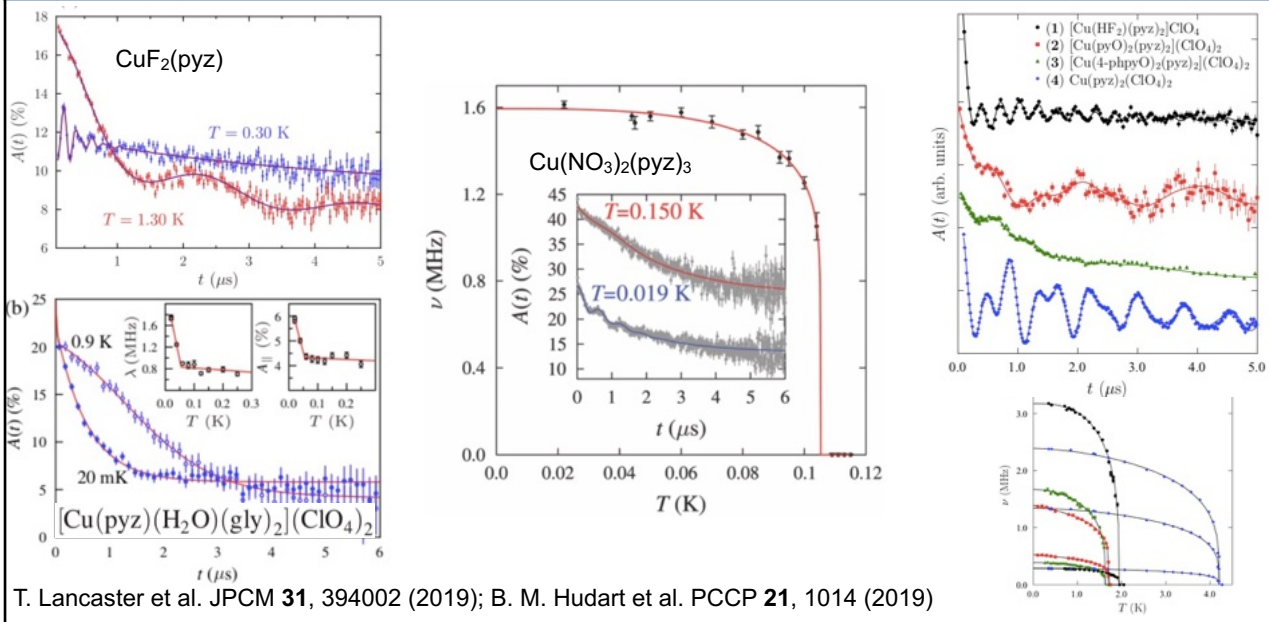

T. Lancaster et al. JPCM **31**, 394002 (2019); B. M. Hudart et al. PCCP **21**, 1014 (2019)
P. A. Goddard et al. Phys. Rev. B **93**, 094430 (2016); T. Lancaster et al. Phys. Rev. Lett. **112**, 207201 (2014)

59

The F-μ-F state

1. Interaction with a single fluorine ion **2**. Crooked FμF bond close to a PF_6^- ion **3**. Interaction with a HF_2^- ion

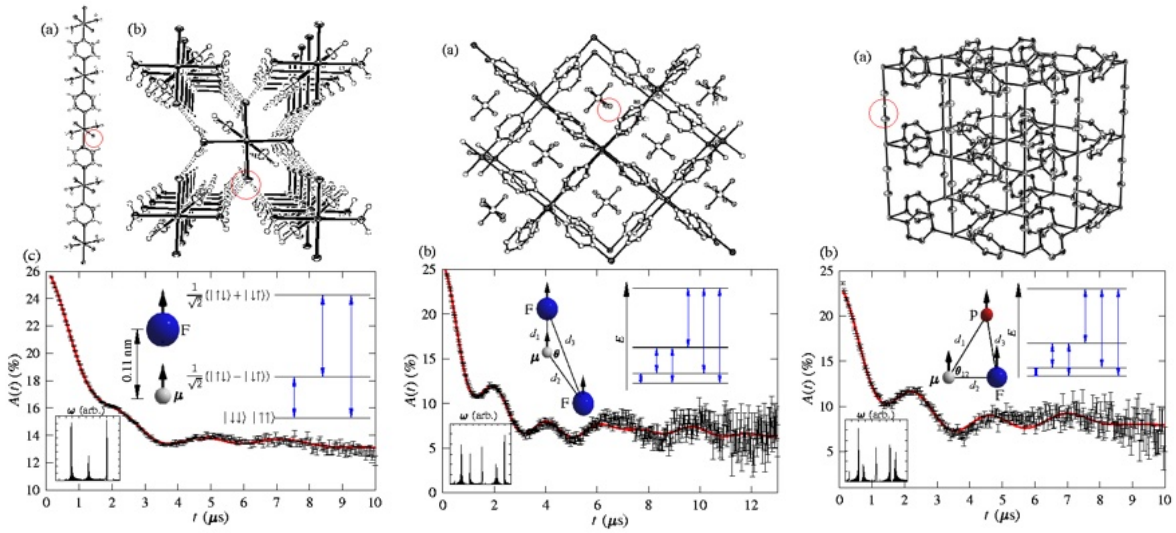

$CuF_2(H_2O)_2(pyz)$ $[CuNO_3(pyz)_2]PF_6$ $[Cu(HF_2)(pyz)_2]X$

T. Lancaster et al. Phys. Rev. Lett. **99**, 267601 (2007)

60

The muon site problem

μSR experiments can be hindered by lack of knowledge of the location of the muon site.

$$B^{\alpha}_{\mathrm{dip}}(\mathbf{r}_\mu) = \sum_i D_i^{\alpha\beta}(\mathbf{r}_\mu) m_i^{\beta} \qquad D_i^{\alpha\beta}(\mathbf{r}_\mu) = \frac{\mu_0}{4\pi R_i^3}\left(\frac{3R_i^\alpha R_i^\beta}{R_i^2} - \delta^{\alpha\beta}\right)$$

$$\mathbf{R}_i \equiv (R_i^x, R_i^y, R_i^z) = \mathbf{r}_\mu - \mathbf{r}_i$$

KEY QUESTIONS:

- Does the muon cause a significant local perturbation?
- Can this change the physics that is probed?

This problem is particularly severe with delicate ground states, such as spin liquids, or those that appear in frustrated systems.

61

Muon sites

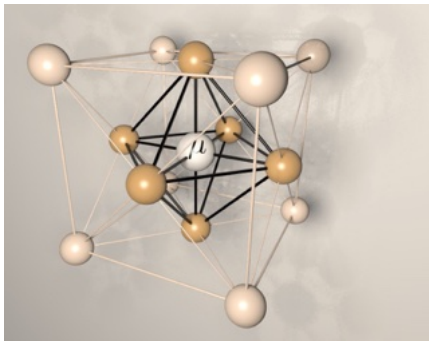

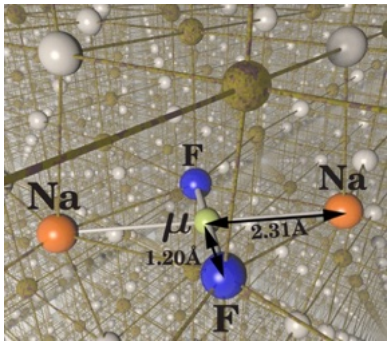

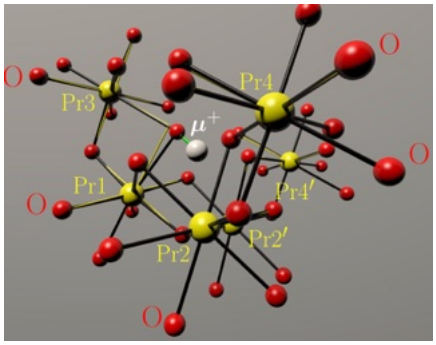

fcc Cu – interstitial site **NaF** – muon between two F^- ions **oxide** – muon bonds to O^{2-} ions

DFT + μ: Density functional theory for muon site determination

- Consider supercell of structure
- Add muon (H pseudopotential) in random site
- Relax the structure, including the muon position
- Evaluate energy. Repeat, for many trial random sites, until minimum energy configuration found.

J. S. Möller, D. Ceresoli, T. Lancaster, N. Marzari and S.J. Blundell, Phys. Rev. B **87**, 121108(R) (2013)
S. J. Blundell and T. Lancaster, Appl. Phys. Rev. **10,** 021316 (2023)

62

MnO – a prototypical antiferromagnet with the NaCl structure

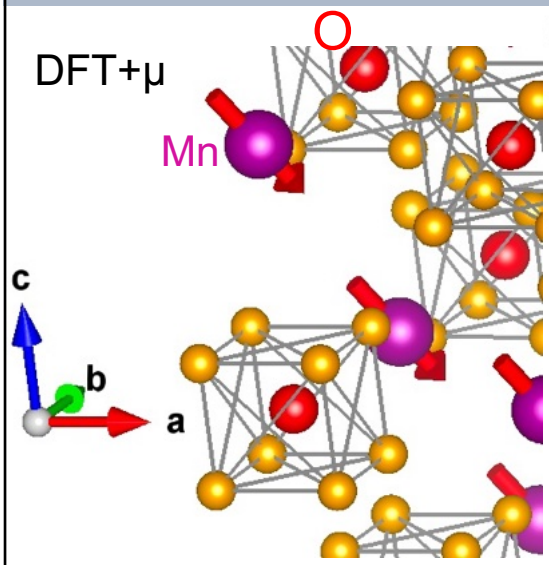

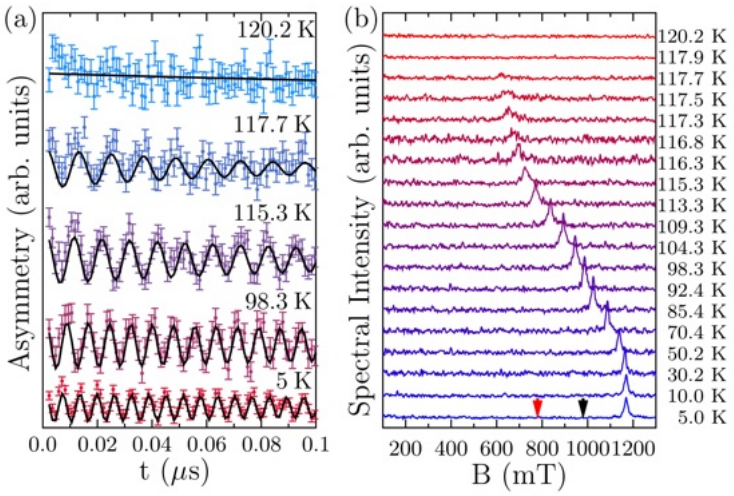

Muon sites (32f) form cubes around O^{2-} ion. But local fields all different, leading to multiple frequencies.

P. Bonfà, I. J. Onuorah, F. Lang, I. Timrov, L. Monacelli, C. Wang, X. Sun, O. Petracic, G. Pizzi, N. Marzari, S. J. Blundell, and R. De Renzi, Phys. Rev. Lett. **132,** 046701 (2024)

63

MnO – a prototypical antiferromagnet with the NaCl structure

$T<T_N$: Rhombohedral distortion $Fm\bar{3}m \rightarrow R3m$ 2c sites more stable (6h sites unstable) implying a single muon precession signal

$T>T_N$: Cubic phase ($Fm\bar{3}m$) and 6h sites are very slightly (32 meV) now lower in energy.

Difference in site stability is driven by magnetostrictive distortion which lifts the degeneracy between the sites. This is **magnetostricton-driven muon localization**.

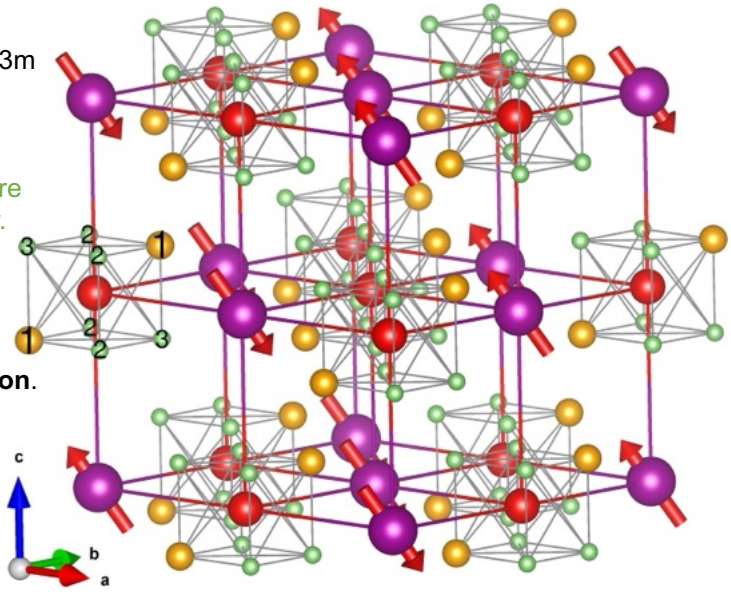

P. Bonfà, I. J. Onuorah, F. Lang, I. Timrov, L. Monacelli, C. Wang, X. Sun, O. Petracic, G. Pizzi, N. Marzari, S. J. Blundell, and R. De Renzi, Phys. Rev. Lett. **132,** (2024)

64

The muon site problem

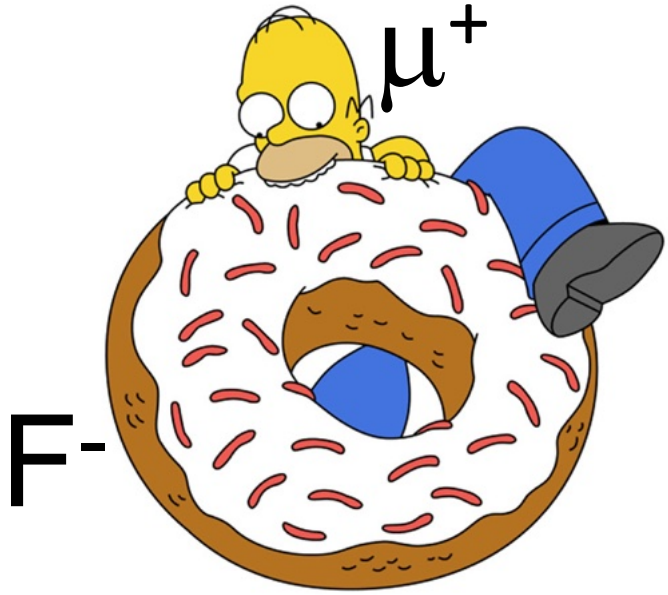

66

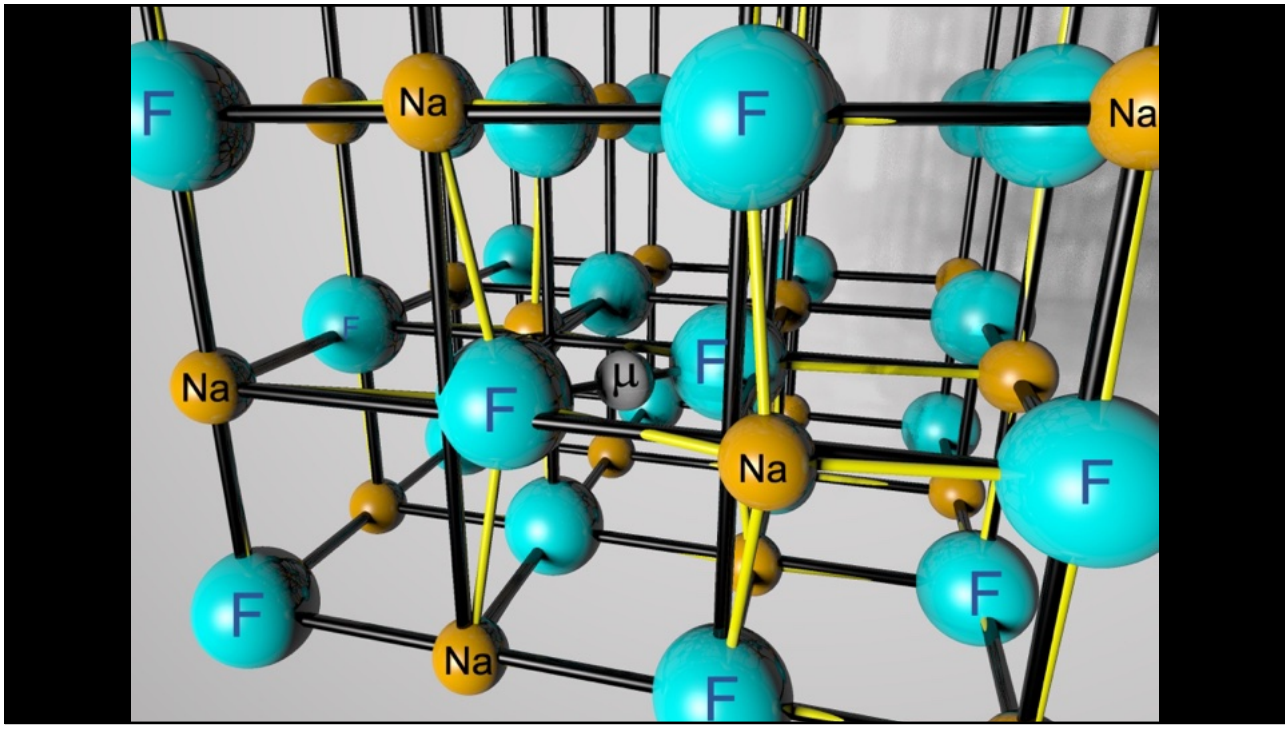

67

Naïve prediction for NaF

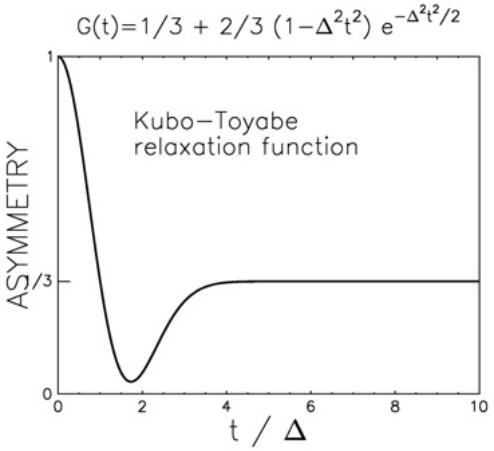

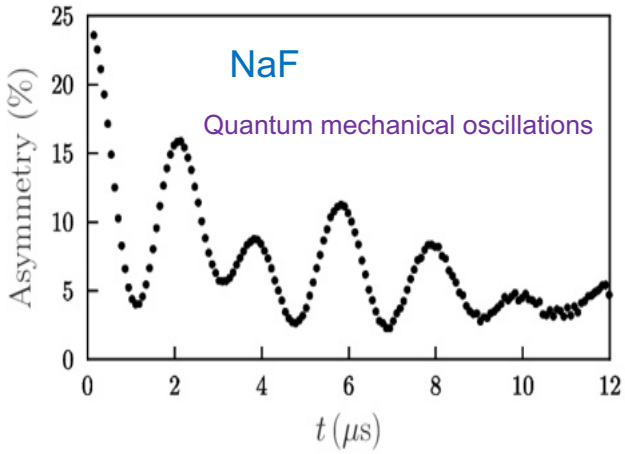

68

Muon fully spin-polarized and so in a **pure** state: $\rho_\mu = \frac{1}{2}(1+\sigma_\mu^z)$

All other nuclei are unpolarized (B=0) and so are in a **mixed** state: $\rho_{\text{nuclei}} = \frac{1}{2^N}$

Muon polarization can be calculated from the time-evolution of the density matrix:

$$\underset{\alpha=x,z}{P_\alpha(t)} = \frac{1}{2^{N+1}}\mathrm{Tr}(\sigma_\mu^\alpha U(t)(1+\sigma_\mu^z)U(t)^\dagger)$$

$$= \frac{1}{2^{N+1}}\sum_{m,n}\langle m|\sigma_\mu^\alpha|n\rangle\langle n|\sigma_\mu^z|m\rangle e^{i\omega_{mn}t}$$

$$\text{For } \alpha = z, P_z(t) = \sum_{m>n} A_{mn}\cos(\omega_{mn}t)$$

69

The F-μ-F state

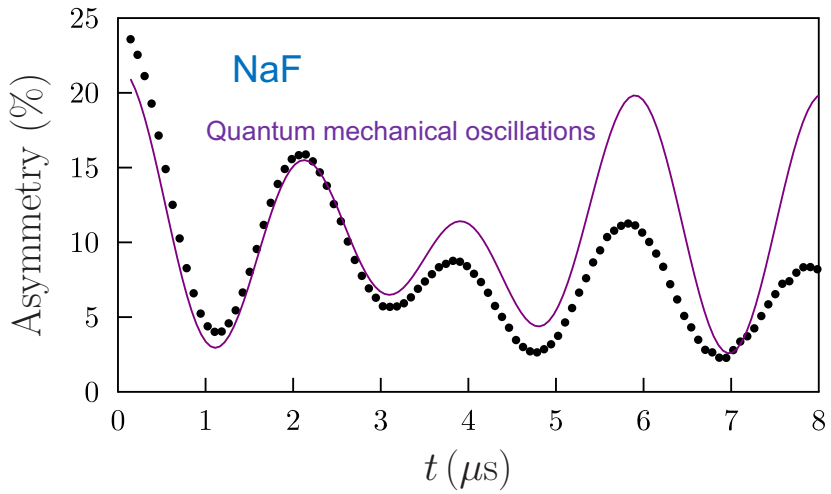

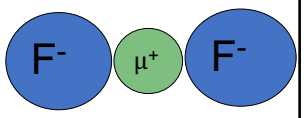

coherent oscillations arising from the magnetic dipolar interaction

$$P_z(t) = \frac{1}{6}\left(3 + \cos\sqrt{3}\omega t + \left(1 - \frac{1}{\sqrt{3}}\right)\cos\left[\frac{3-\sqrt{3}}{2}\omega t\right] + \left(1 + \frac{1}{\sqrt{3}}\right)\cos\left[\frac{3+\sqrt{3}}{2}\omega t\right]\right)$$

70

The F-μ-F state

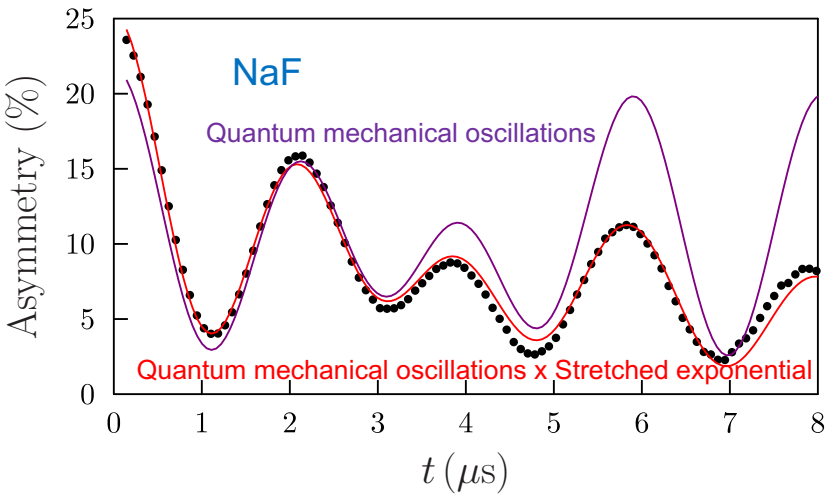

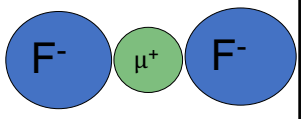

coherent oscillations arising from the magnetic dipolar interaction

Stretched exponential

$$P_z(t) = \frac{1}{6}\left(3 + \cos\sqrt{3}\omega t + \left(1 - \frac{1}{\sqrt{3}}\right)\cos\left[\frac{3-\sqrt{3}}{2}\omega t\right] + \left(1 + \frac{1}{\sqrt{3}}\right)\cos\left[\frac{3+\sqrt{3}}{2}\omega t\right]\right) \times e^{-(\lambda t)^{\beta}}$$

71

The F-μ-F state

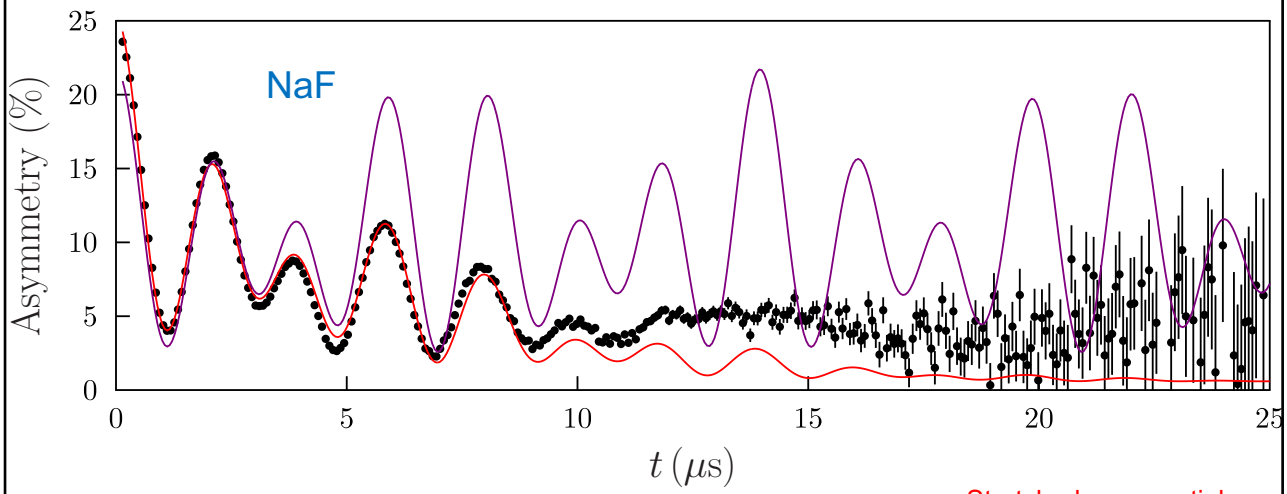

Stretched exponential

$$P_z(t) = \frac{1}{6}\left(3 + \cos\sqrt{3}\omega t + \left(1 - \frac{1}{\sqrt{3}}\right)\cos\left[\frac{3-\sqrt{3}}{2}\omega t\right] + \left(1 + \frac{1}{\sqrt{3}}\right)\cos\left[\frac{3+\sqrt{3}}{2}\omega t\right]\right) \times e^{-(\lambda t)^{\beta}}$$

72

CaF_2

99.9% of Ca have zero nuclear spin

fluorite structure

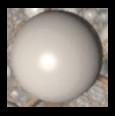

fluorine

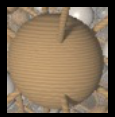

calcium

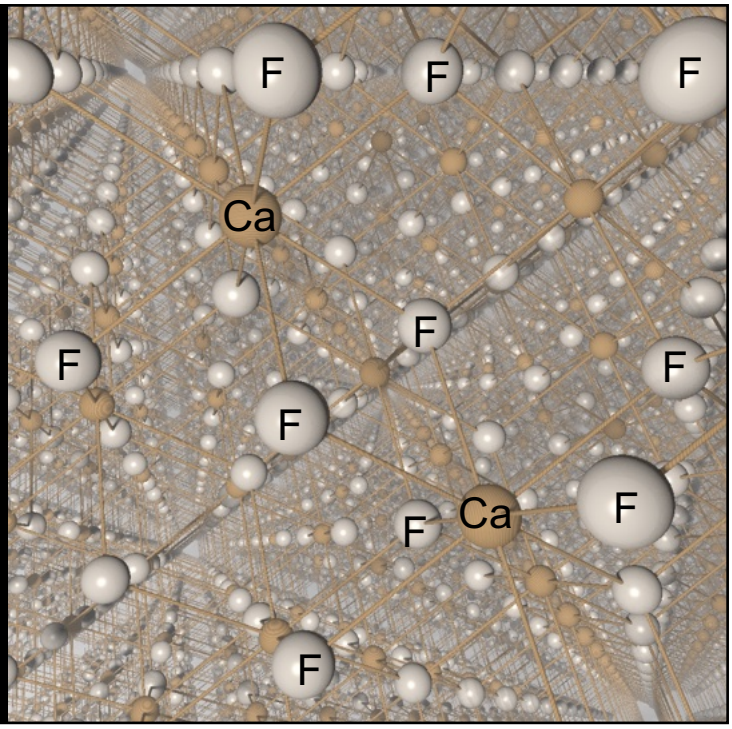

73

CaF_2

99.9% of Ca have zero nuclear spin

fluorite structure

fluorine

calcium

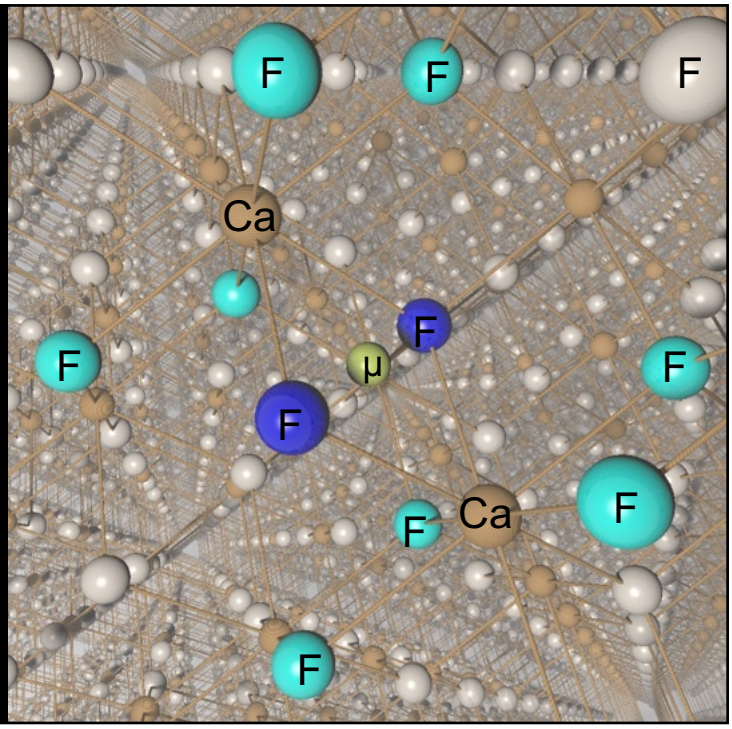

74

CaF_2

99.9% of Ca have zero nuclear spin

fluorite structure

Muon + two nn F:
Hamiltonian 8 x 8

Muon + two nn F + eight nnn F:
Hamiltonian 2048 x 2048

fluorine

calcium

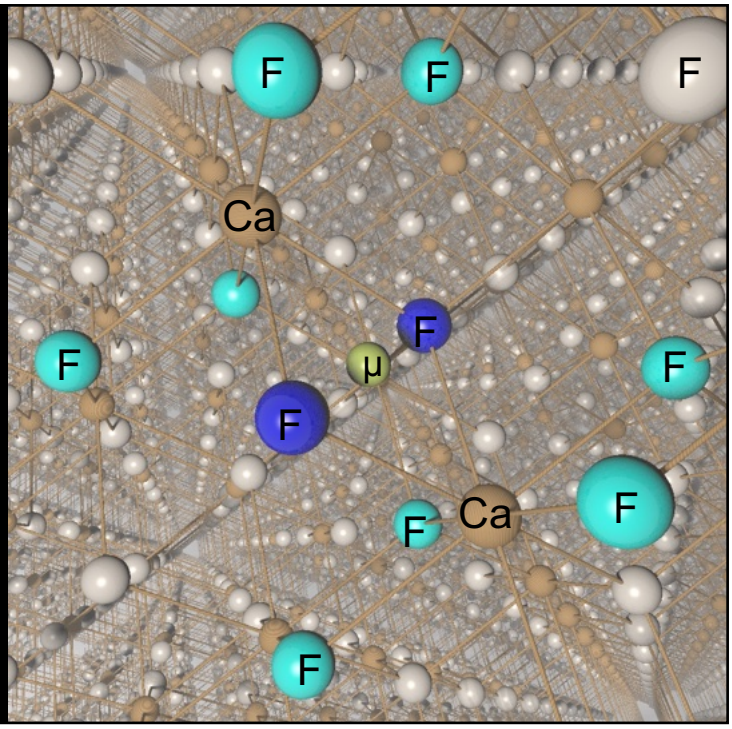

75

The F-μ-F state – only nn interactions

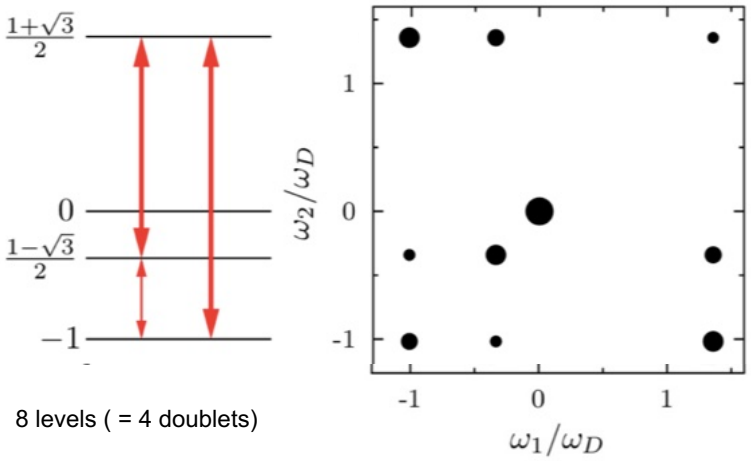

8 levels (= 4 doublets)

Reminiscent of a
COSY plot in 2D NMR

J. M. Wilkinson and S. J. Blundell, Phys. Rev. Lett. **125**, 087201 (2020)

76

The F-μ-F state – nn and nnn interactions

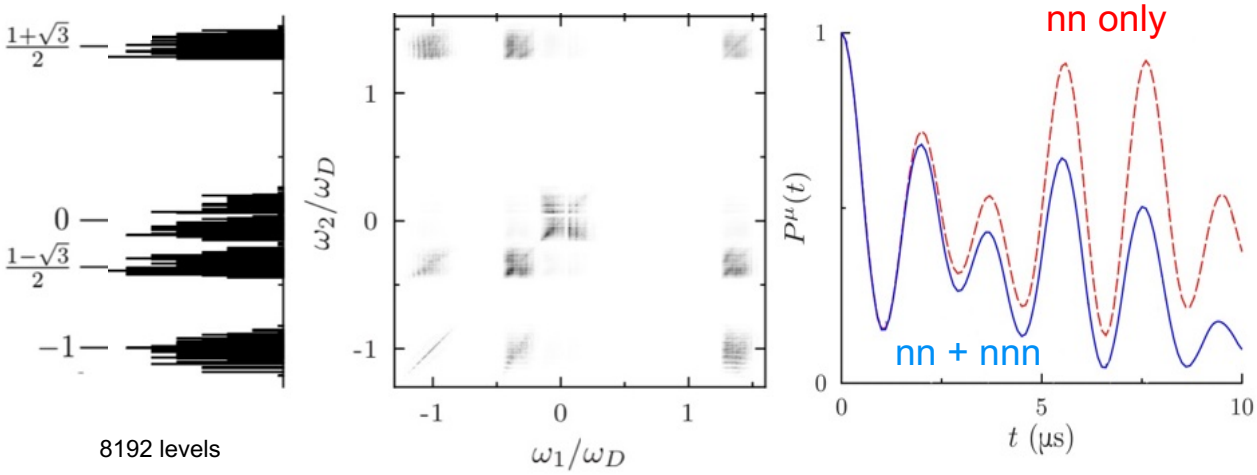

8192 levels

- Muon implanted with 1 “qubit” of quantum information
- In a finite isolated system, the qubit rattles around and the entropy oscillates back and forth
- With additional interactions, the quantum information decoheres through the system and the muon entropy rises.

J. M. Wilkinson and S. J. Blundell, Phys. Rev. Lett. **125**, 087201 (2020)

77

CaF_2

fluorite structure

fluorine

calcium

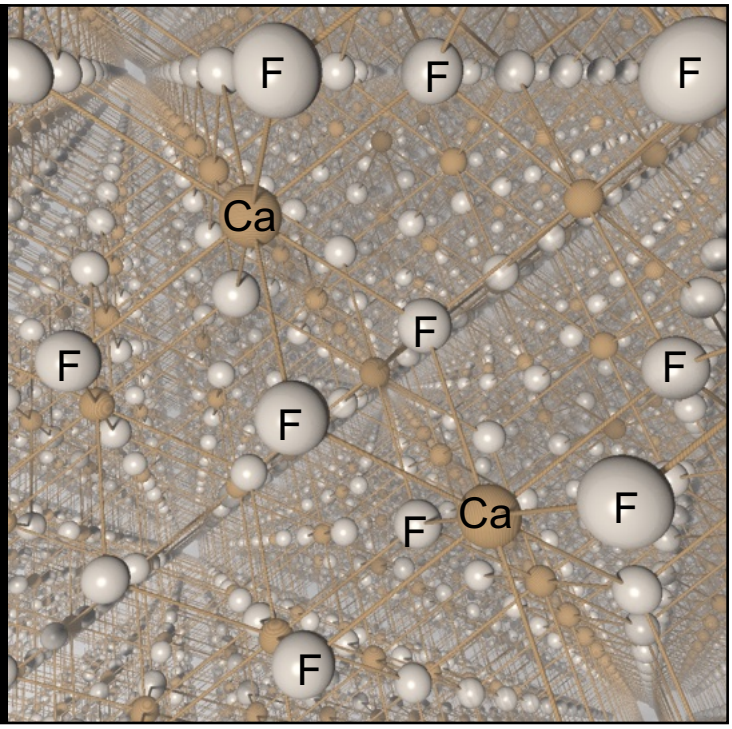

78

CaF_2

fluorite structure

fluorine

calcium

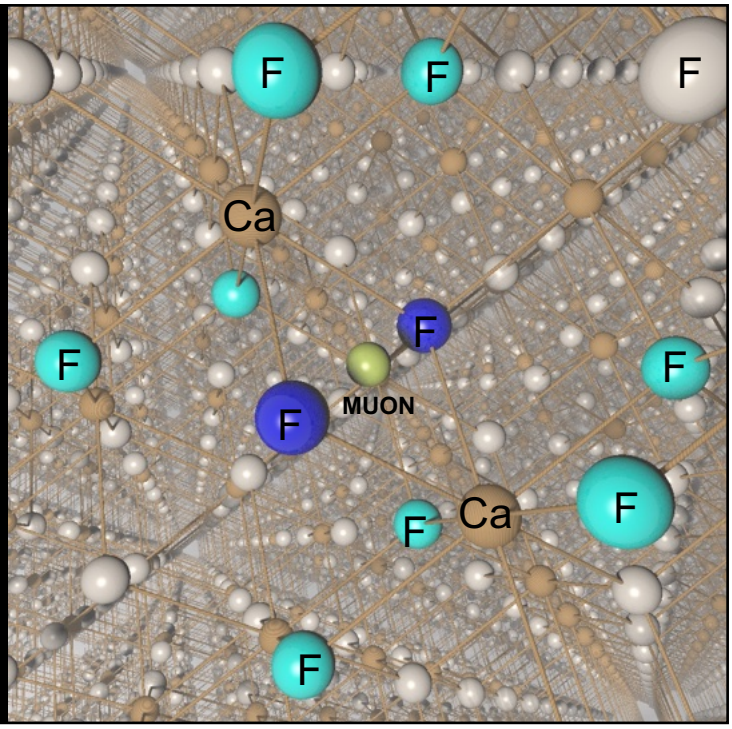

79

CaF_2

fluorite structure

fluorine

calcium

DFT+μ

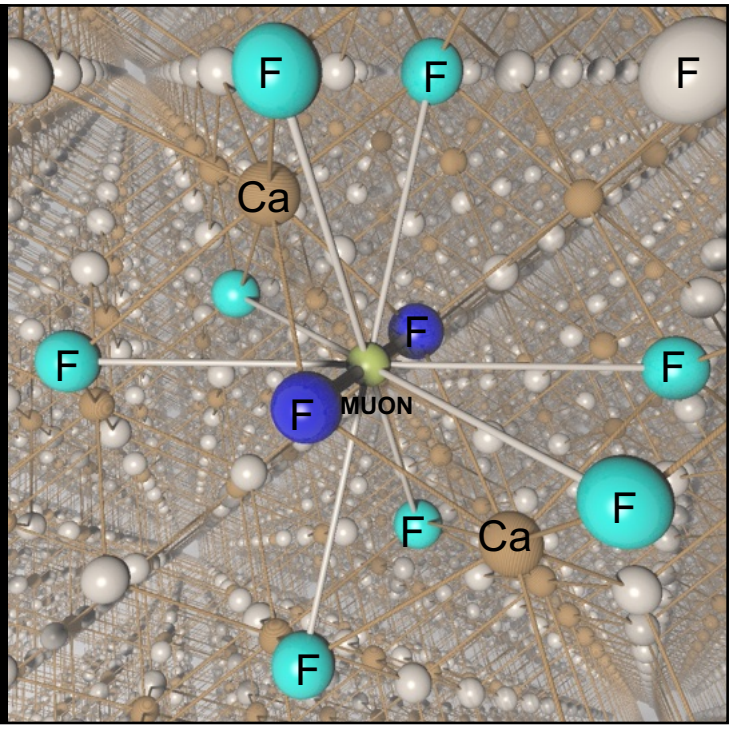

80

NaF

NaCl structure

fluorine

sodium

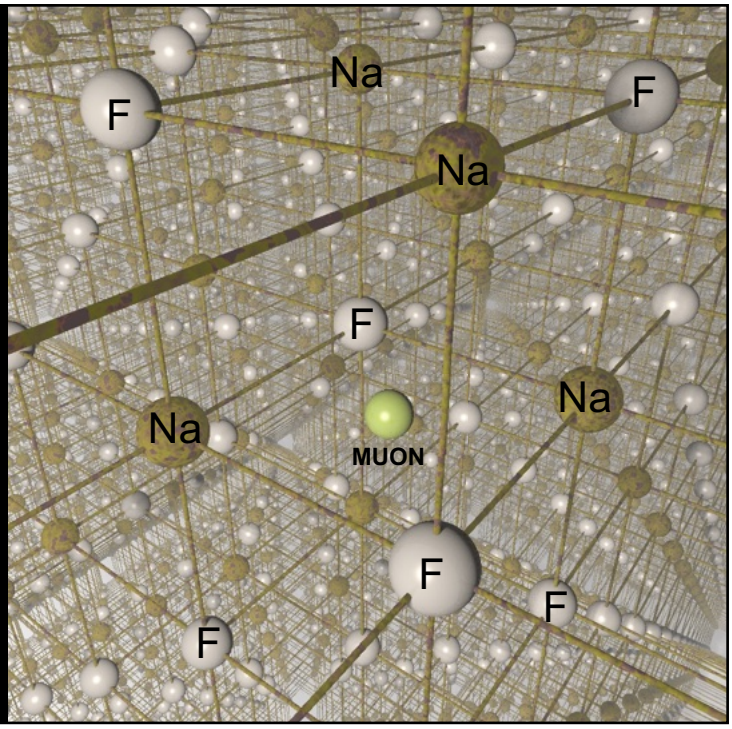

81

NaF

NaCl structure

fluorine

sodium

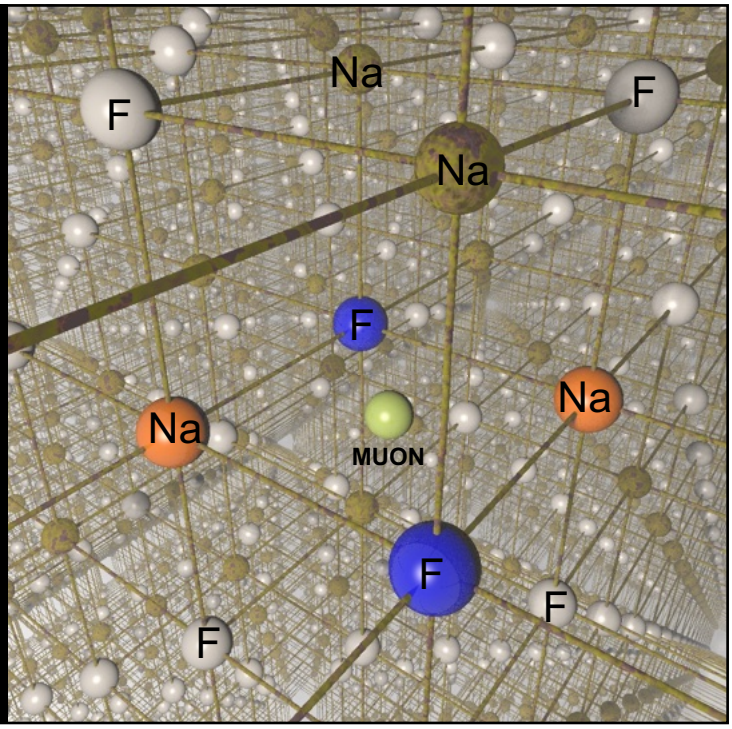

82

NaF

NaCl structure

fluorine

sodium

DFT+μ

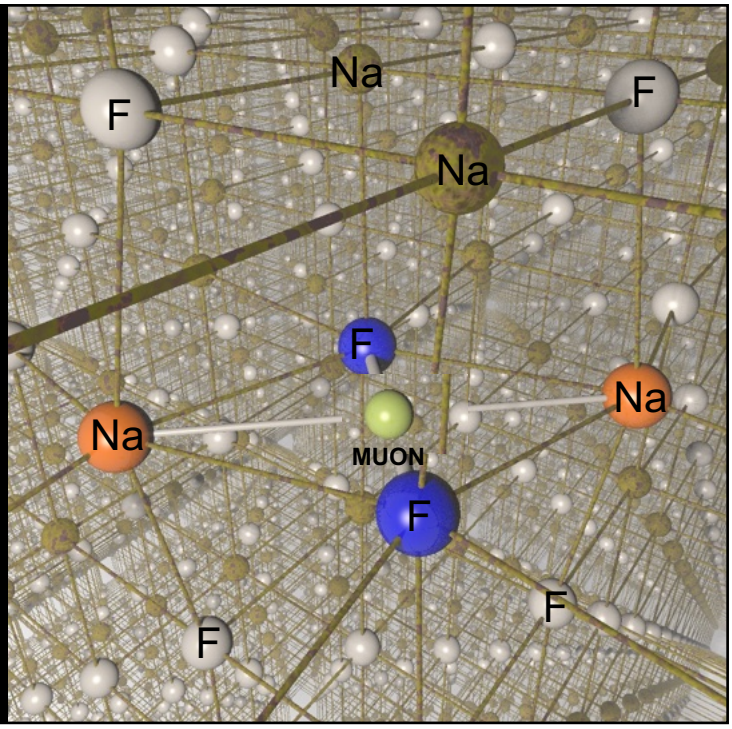

83

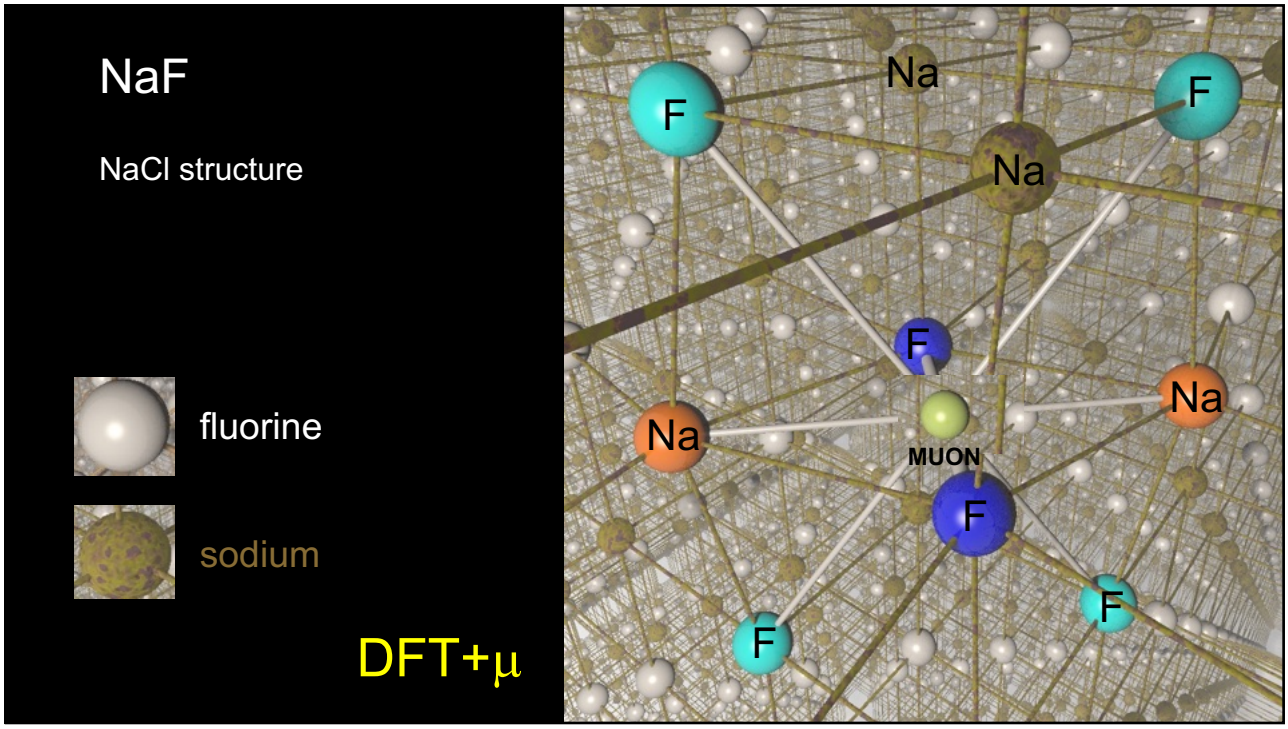

84

Fluoride nuclear-muon coupling and decoherence

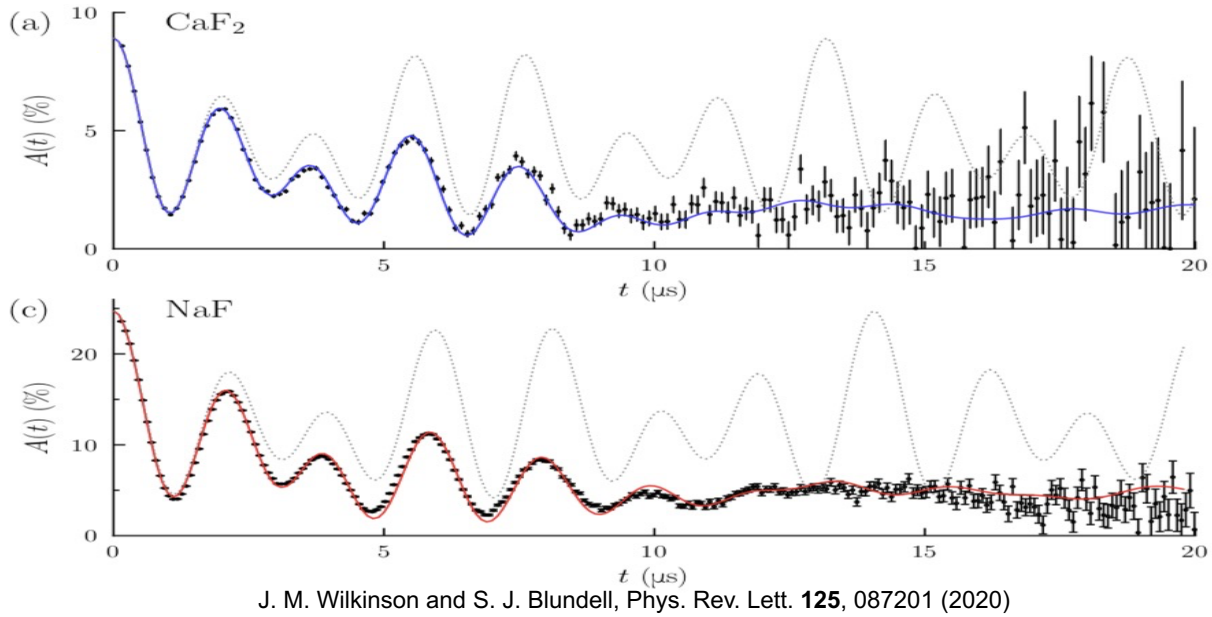

J. M. Wilkinson and S. J. Blundell, Phys. Rev. Lett. **125**, 087201 (2020)

85

Relaxation of oscillations is sensitive to the site

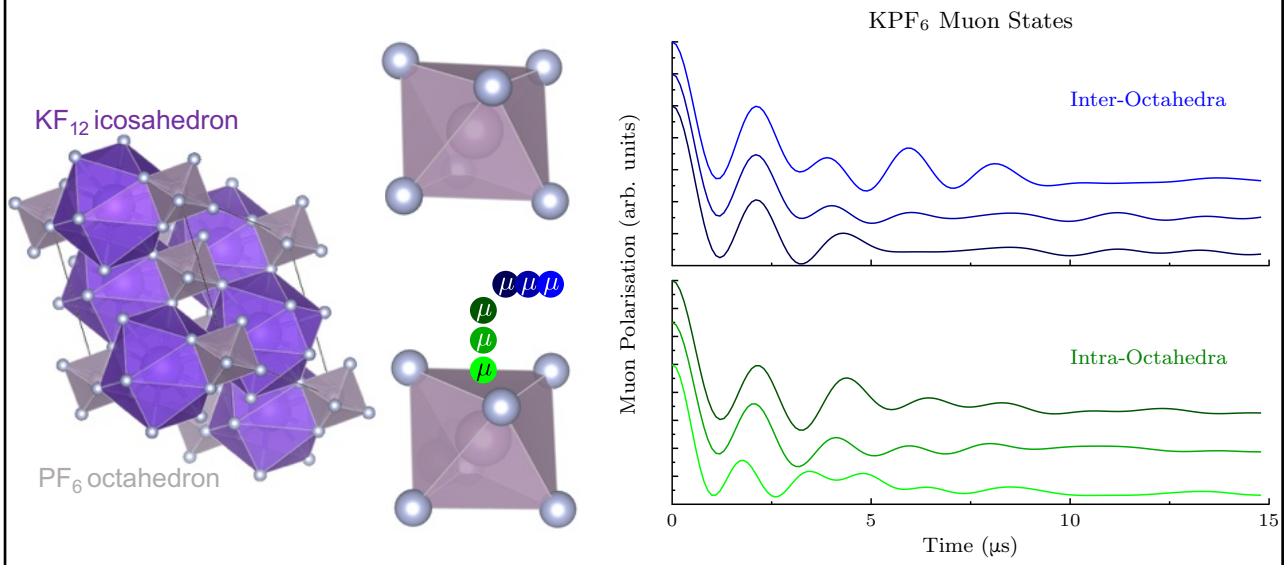

J. M. Wilkinson *et al.,* J. Phys.: Conf. Ser. **2462**, 012007 (2023)
see also J. M. Wilkinson, F. L. Pratt, T. Lancaster, P. J. Baker, and S. J. Blundell, Phys. Rev. B **104**, L220409 (2021) for PbF_2 and YF_3

86

Magnetism and muon sites in Cs_2AgF_4

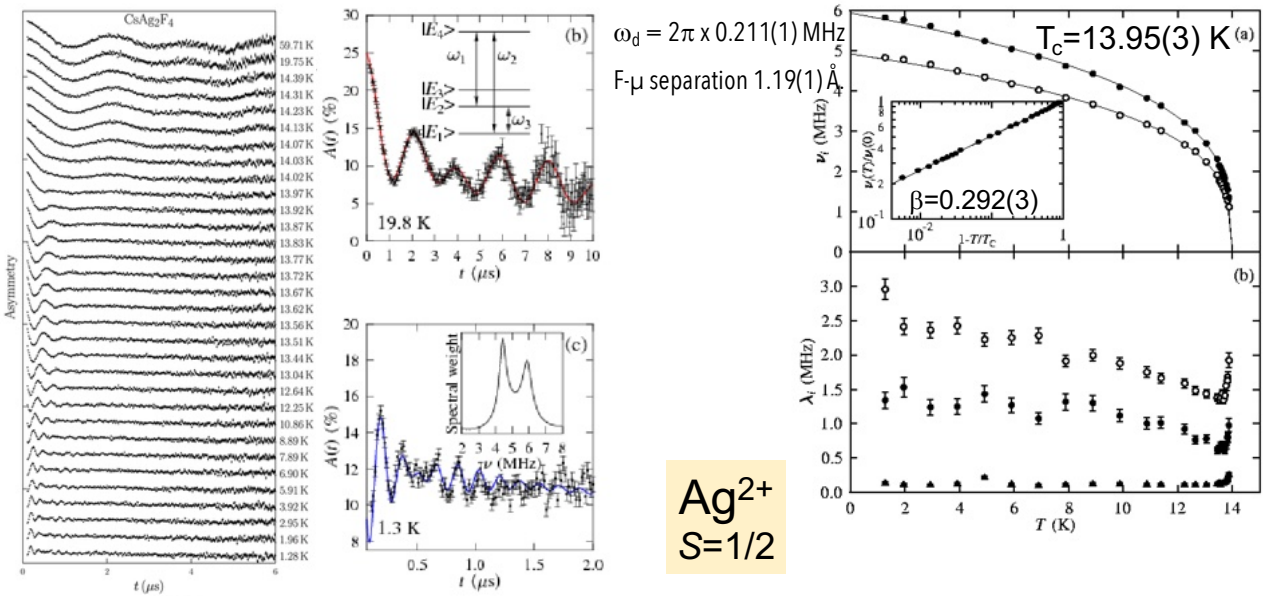

T. Lancaster, S. J. Blundell, et al. Phys. Rev. B **75**, R220408 (2007)

87

Quasi-one-dimensional magnet $KAgF_3$

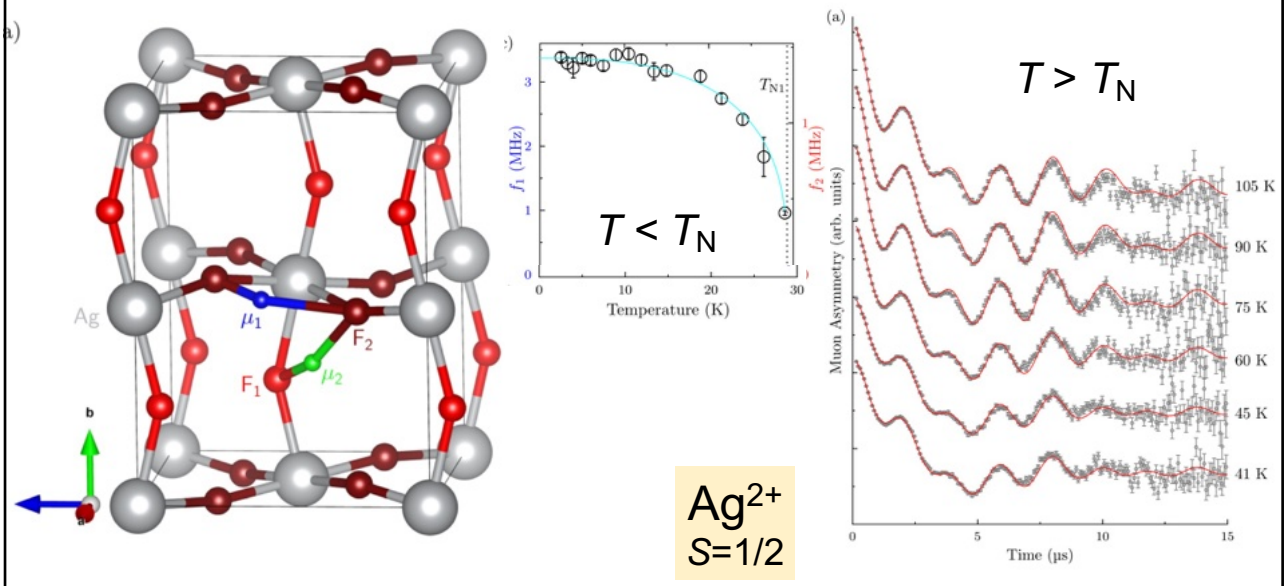

Ag^{2+}
S=1/2

J. M. Wilkinson, S. J. Blundell, S. Biesenkamp, M. Braden, T. C. Hansen, K. Koteras, W. Grochala, P. Barone, J. Lorenzana, Z. Mazej, and G. Tavcar, Phys. Rev. B **107**, 144422 (2023)

88

RF techniques – LaF_3

B_0 = 9.6 mT,

1.32 MHz continuous wave radiofrequency irradiation

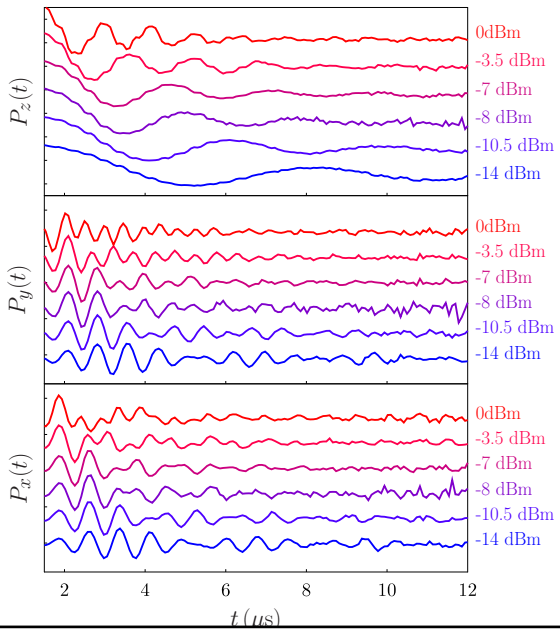

RF power, which increases B_1

89

RF techniques – LaF_3

B_0 = 9.6 mT,

1.32 MHz continuous wave radiofrequency irradiation

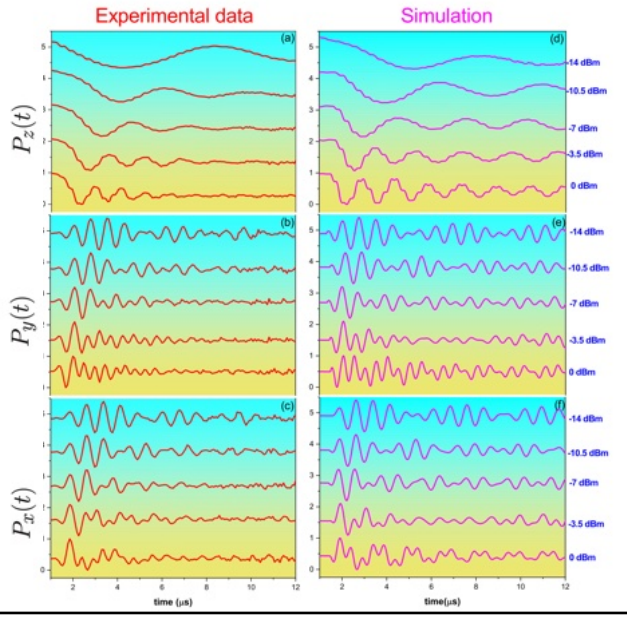

RF power, which increases B_1

90

Longitudinal field – spectral density $J(\omega)$ of spin fluctuations

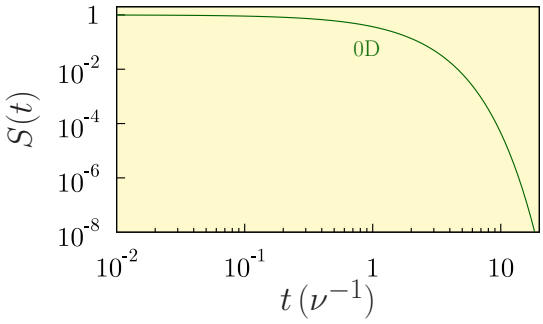

Uncorrelated spins

$$S_{0D}(t) = \exp(-\nu t)$$

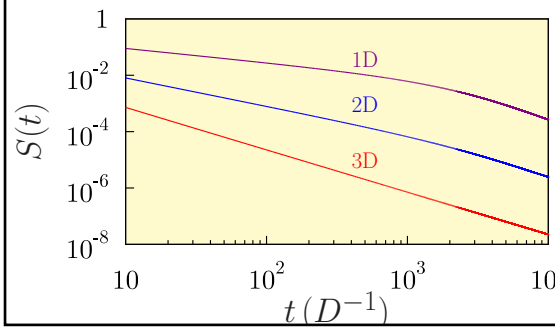

Diffusion on an anisotropic lattice

$$S(t) = \prod_{i=1}^{3} \exp(-2D_i t) I_0(2D_i t)$$

F. L. Pratt, F. Lang, S. J. Blundell, W. Steinhardt, S. Haravifard, S. Mañas-Valero, E. Coronado, B. M. Huddart and T. Lancaster, J. Phys.: Conf. Ser. 2462, 012038 (2023)

91

Longitudinal field – spectral density $J(\omega)$ of spin fluctuations

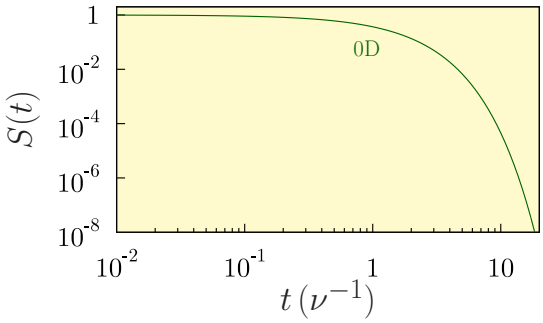

Uncorrelated spins

$$S_{0D}(t) = \exp(-\nu t)$$

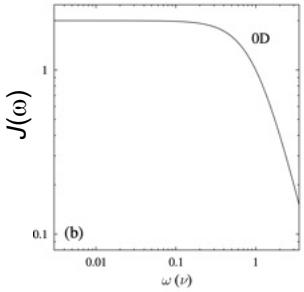

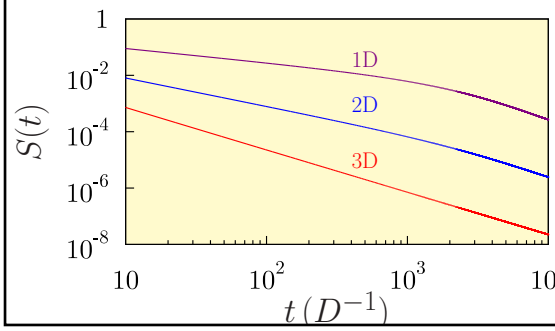

Diffusion on an anisotropic lattice

$$S(t) = \prod_{i=1}^{3} \exp(-2D_i t) I_0(2D_i t)$$

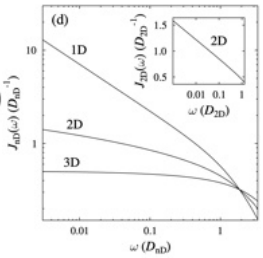

F. L. Pratt, F. Lang, S. J. Blundell, W. Steinhardt, S. Haravifard, S. Mañas-Valero, E. Coronado, B. M. Huddart and T. Lancaster, J. Phys.: Conf. Ser. 2462, 012038 (2023)

92

$YbZnGaO_4$ and $YbZn_2GaO_5$

$YbZnGaO_4$

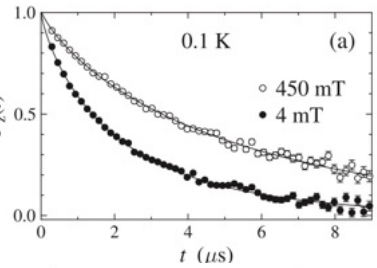

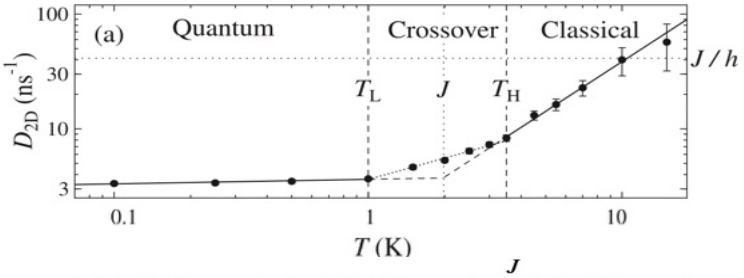

$YbZn_2GaO_5$

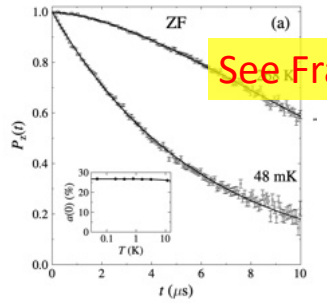

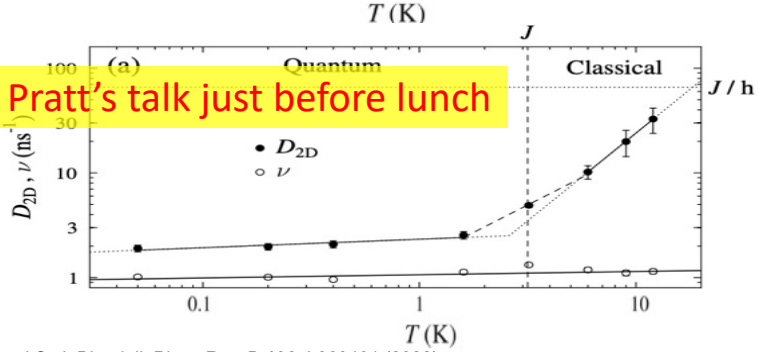

See Francis Pratt's talk just before lunch

$YbZnGaO_4$: F. L. Pratt, F. Lang, W. Steinhardt, S. Haravifard and S. J. Blundell, Phys. Rev. B **106**, L060401 (2022)
$YbZn_2GaO_5$: H. C. H. Wu, F. L. Pratt, B. M. Huddart, D. Chatterjee, P. A. Goddard, J. Singleton, D. Prabhakaran, S. J. Blundell, arXiv 2502.00130

93

Summary

- Muon sites have been determined for alkali halides. They show an interesting dependence on the details of the structure. Nuclear spin environments can be fitted in detail.
- In fluorine-containing molecular magnets, muon sites can be studied and characterized and the new DFT+μ techniques are revealing the (sometimes unexpected) stopping state of the implanted muon, and even its propensity to perform chemical reactions.
- We still lack a quantitative understanding of persistent spin dynamics in spin liquids. A key experimental advance to to solve this will be the development of double resonance techniques that combine μSR, NMR and ESR.

94